Journal of the Geological Society, London, Vol. **161**, 2004, pp. 447–462. Printed in Great Britain.

Age of the Ballachulish and Glencoe Igneous Complexes (Scottish Highlands), and paragenesis of zircon, monazite and baddeleyite in the Ballachulish Aureole

G.L. FRASER[1,2], D.R.M. PATTISON[1] & L.M. HEAMAN[3]

[1]*Department of Geology and Geophysics, University of Calgary, Calgary, Alberta T2N 1N4, Canada*

[2]*Present address: Geoscience Australia, GPO Box 378, Canberra, A.C.T. 2601, Australia, and Research School of Earth Sciences, Australian National University, Acton, A.C.T. 0200, Australia (e-mail: Geoff.Fraser@ga.gov.au)*

[3]*Department of Earth and Atmospheric Sciences, University of Alberta, Edmonton, Alberta T6G 2E3, Canada*

Abstract: U–Pb zircon ages are presented for the Ballachulish Igneous Complex (^{207}Pb–^{206}Pb age 427 ± 1 Ma; ^{206}Pb–^{238}U age 423 ± 0.3 Ma) and Glencoe Volcanic Complex (^{207}Pb–^{206}Pb age 406 ± 6 Ma) of the Scottish Highlands. These ages are significantly more precise than pre-existing age constraints, and discriminate a previously unresolved age difference of *c*. 20 Ma between the two complexes. This difference in age provides an explanation for the *c*. 10 km difference in crustal level between the two magmatic events, and constrains exhumation rates for the Argyll region to be on average *c*. 0.4 km Ma^{-1} over the period *c*. 425–405 Ma. With improved age constraints on the Ballachulish Igneous Complex in place, the associated metamorphic aureole is used as a type locality to investigate the metamorphic behaviour of the U-bearing accessory minerals baddeleyite, zircon and monazite. Baddeleyite formed in impure dolomites by the reaction of detrital zircon with dolomite and gives the same U–Pb age as the intrusive complex, consistent with its contact metamorphic origin. Detrital zircon appears to be inert throughout much of the metamorphic aureole, with contact metamorphic zircon growth being restricted to migmatite-grade rocks. A possible exception is the development of enigmatic, very narrow overgrowths at temperatures between *c*. 500 and 600 °C. Monazite exhibits a variety of textures in lower-grade parts of the aureole (<550 °C), but occurs as distinctive clusters and trails of tiny ovoid grains at temperatures above about 560–600 °C. Monazite thus appears sensitive to metamorphism at lower temperatures than zircon and may therefore be a better target for metamorphic age measurements in rocks that reach mid-amphibolite facies but do not experience partial melting.

Keywords: Ballachulish Complex, Glencoe, baddeleyite, zircon, monazite.

The Ballachulish and Glencoe Igneous Complexes are both classic geological localities; Ballachulish as an example of a zoned igneous pluton with a well-preserved metamorphic aureole (Voll *et al*. 1991; Pattison & Harte 1997), and Glencoe being the original type example of volcanic caldera collapse (Clough *et al*. 1909). Despite a long history of geological investigation, Caledonian igneous and metamorphic events in the Scottish Highlands are subject to relatively few precise radiometric age constraints (e.g. Rogers & Dunning 1991; Stewart *et al*. 2001), and this has limited tectonic understanding of the region. In this paper we present precise U–Pb zircon age constraints for late Caledonian magmatism at Ballachulish and Glencoe that reconcile contrasting geological features of the two igneous complexes. We then use the Ballachulish aureole to investigate the behaviour of zircon, monazite and baddeleyite in a well-constrained metamorphic setting. These observations contribute to an understanding of the metamorphic response of these minerals that is critical to meaningful interpretation of U–Pb ages from metamorphic rocks.

Geological setting and previous age constraints for the Ballachulish Igneous Complex and Glencoe Volcanic Complex

Both the Ballachulish and Glencoe Igneous Complexes are products of late Caledonian magmatism, which affected much of the Scottish Highlands, Ireland, Scandinavia, eastern Greenland and eastern North America. A comprehensive description of late Caledonian magmatism in the Grampian Highlands has been given by Stephenson & Gould (1995). Late Caledonian magmatism in Scotland spans a period in which deformation along the Great Glen Fault and related strike-slip structures was occurring, probably related to closure of the Iapetus ocean (Thirlwall 1988; Rogers & Dunning 1991; Stewart *et al*. 1999). Contrasting interpretations for the genesis of the late Caledonian magmas have been proposed, with at least some of the debate hinging on timing of magmatism relative to subduction across the Iapetus suture. Thirlwall (1988) attempted to subdivide Caledonian magmatic activity according to geological province and age, but the vast majority of the geochronological data at that time were Rb–Sr mineral ages with relatively large uncertainties, which made tectonic interpretation difficult. More recently, high-precision U–Pb data for a small number of late Caledonian plutons (Rogers & Dunning 1991) have underscored the uncertainty associated with some of the earlier datasets.

The only pre-existing radiometric age constraints for the Ballachulish Igneous Complex come from four K–Ar mineral ages (Miller & Brown 1965; Brown *et al*. 1968), which range from 387 ± 6 Ma to 420 ± 19 Ma, and two Rb–Sr whole-rock isochrons reported by Haslam & Kimbell (1981), which give ages of 406 ± 34 Ma and 418 ± 77 Ma. The range in reported ages and the relatively poor precision on each, coupled with the well-established susceptibility to resetting of both the K–Ar and Rb–Sr systems, leaves considerable uncertainty on the intrusive age. Weiss (1986) averaged these published ages to yield a value of 412 ± 28 Ma, which has since been used as the best estimate

for emplacement age for the Ballachulish Igneous Complex (e.g. Voll *et al*. 1991; Pattison & Harte 1997).

Age constraints for the Glencoe Volcanic Complex are similarly poor, with the only direct age determinations coming from two $^{40}Ar/^{39}Ar$ step heating experiments on hornblende separated from Glencoe andesite (Thirlwall 1988). One of these two experiments yields a relatively well-defined plateau in which 86% of the gas is released in six consecutive steps with a combined age of 421 ± 4 Ma. The other experiment was a very coarse step-heat consisting of only three temperature steps and dominated by a step containing 92% of the gas with an age of 413 ± 0.5 Ma. No details were given of the standard used for monitoring neutron fluence, or the age assigned to the standard.

A minimum age constraint on the Glencoe Volcanic Complex could be provided by the cross-cutting Etive dykes; however, no direct age determinations exist for these dykes. The best constraints for the dykes come from Rb–Sr whole-rock isochrons from the Cruachan and Starav granites, which respectively are cut by, and cross-cut the Etive dykes. Ages from these granites bracket the time of dyke intrusion between 401 ± 6 Ma and 396 ± 12 Ma (Clayburn *et al*. 1983), implying that the Glencoe Volcanic Complex is older than about 400 Ma.

The Ballachulish Igneous Complex

The Ballachulish Igneous Complex and the surrounding metamorphic aureole is one of the world's most extensively studied plutonic–metamorphic complexes (Pattison & Harte 1997). The igneous complex covers an area of *c*. 8×5 km^2 on the southern side of Loch Linnhe near the mouth of Loch Leven (Fig. 1), *c*. 4 km SE of the Great Glen Fault. Detailed descriptions of the igneous complex have been presented by Weiss & Troll (1989) and Voll *et al*. (1991). The Ballachulish Igneous Complex consists of an outer envelope of diorites and monzodiorites and an inner core of granite and granodiorite. The outer diorites and monzodiorites were intruded into Dalradian metasediments at a temperature of *c*. 1100 °C, closely followed by intrusion of the granites and granodiorites at 850–900 °C while the outer diorites were still partially molten (Weiss & Troll 1989). Numerous appinites are found in the vicinity, including some relatively large bodies on the SE margin of the Ballachulish Igneous Complex (Fig. 1). Gradational contacts of these appinites with the adjacent diorites of the Ballachulish Igneous Complex suggest that they were emplaced more or less synchronously with the Ballachulish Igneous Complex (Weiss & Troll 1989). Petro-

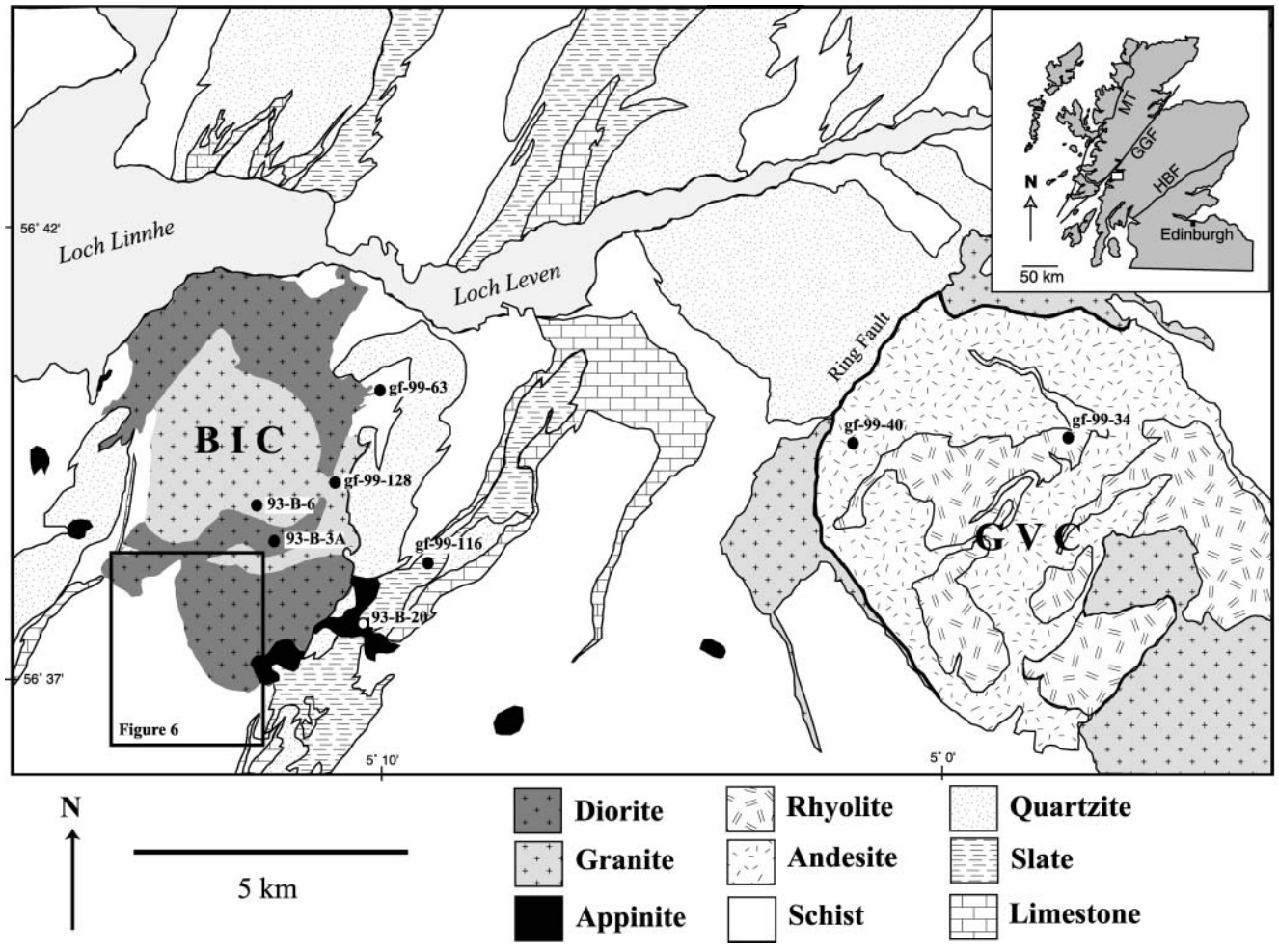

Fig. 1. Simplified geological map of the Ballachulish–Glencoe region showing the Ballachulish Igneous Complex (BIC) and Glencoe Volcanic Complex (GVC) and the localities of samples referred to in the text. The bold square in the SW of the Ballachulish Igneous Complex outlines the region shown in Figure 6. Geology based on Bailey & Maufe (1960) and Pattison & Harte (2001). The inset map shows the locality of the Ballachulish–Glencoe region (open box in inset map) relative to major geological structures in Scotland. MT, Moine Thrust; GGF, Great Glen Fault; HBF, Highland Boundary Fault.

logical evidence indicates that the metamorphic aureole around the Ballachulish Igneous Complex developed at a pressure of *c*. 3 kbar, implying an intrusion depth of *c*. 10 km (Pattison 1989, 1992).

Geology of the Glencoe Volcanic Complex

The Glencoe Volcanic Complex is one of several late Caledonian volcanic ring complexes in the Scottish Highlands that include the Ben Nevis and Etive complexes. The Glencoe Volcanic Complex is situated south of Loch Leven, about 10 km east of the Ballachulish Igneous Complex (Fig. 1). Volcanic rocks are restricted to a roughly circular region of *c*. 8 km in diameter separated from marginal granites and surrounding Dalradian metasediments by a ring fault (Clough *et al*. 1909). Bailey & Maufe (1960) divided the volcanosedimentary sequence into seven groups, with a total thickness of slightly more than 1 km. The basal part of the sequence sits unconformably on Dalradian metasediments and consists of andesitic sheets (Group I of Bailey & Maufe 1960), *c*. 500 m thick. These were originally described as lava flows (Clough *et al*. 1909) but have subsequently been interpreted as sills intruding wet sediment (Moore & Kokelaar 1998). The original interpretation of Clough *et al*. (1909) was that the region inside the ring fault subsided as a coherent block, forming a caldera filled with the volcanosedimentary package. Moore & Kokelaar (1998) presented an alternative view, in which the basal andesites predated caldera development and caldera collapse occurred in multiple stages via movement on several orthogonal faults, which formed a NW-trending graben within the ring fault. Moore & Kokelaar (1998) interpreted the ring fault to have been active late in the volcanic history, and estimated that the total duration of volcanic activity at Glencoe, including the basal andesites, may have been of the order of 1 Ma. Partially encircling the Glencoe Volcanic Complex, and localized around the ring fault, are granites interpreted to have ascended along the ring fault and therefore regarded as broadly synchronous with the volcanic activity. In the SE the Glencoe Volcanic Complex is intruded by the Cruachan Granite.

U–Pb analytical techniques

To provide high-precision age estimates for both the Ballachulish Igneous Complex and Glencoe Volcanic Complex we have applied the thermal ionization mass spectrometric (TIMS) method to small numbers of handpicked zircons and in some cases single zircon grains. Methods follow those described in more detail by Heaman *et al*. (2002). Results are given in Table 1, with uncertainties quoted at 1σ, whereas error ellipses shown in Figures 2, 3 and 5 are 2σ.

Results from the Ballachulish Igneous Complex

Zircons from three samples within the Ballachulish Igneous Complex have been analysed. Samples were selected that bracket the duration of intrusive activity, including an appinite interpreted to closely predate the main diorite intrusion, a typical monzodiorite and a late-stage granite.

93-B-20, appinite

This sample was collected from the southeastern part of the Ballachulish Igneous Complex (Fig. 1), where appinitic rocks crop out over an area of several hundred square metres. This appinitic body has been mapped as a mafic stock but has complex, gradational relationships with the adjacent diorites of the Ballachulish Igneous Complex, which suggest that it closely predates the diorites (Troll & Weiss 1991). The sample contains an igneous assemblage of plagioclase, clinopyroxene, biotite and minor K-feldspar. Accessory phases include apatite, rutile, titanite and zircon.

Zircon from this sample is modally rare and falls into two morphological categories: (1) elongate needles with aspect ratios >5; (2) relatively equant grains. Both morphological types exhibit well-formed crystal faces. Five zircon fractions from this sample were analysed (Fig. 2a). Four zircon fractions include both needle-like zircon as well as equant, stubby grains. At the 2σ level of uncertainty these four fractions overlap and three of the four fall within error of concordia. The weighted-mean $^{206}Pb–^{238}U$ age for these four fractions 1, 3, 4 and 5 is 420 ± 0.1 Ma, with a χ^2 value of 4.92, suggesting slight excess scatter. It could be argued that fractions 4 and 5 have suffered minor Pb loss, making the best estimate $^{206}Pb–^{238}U$ age 422 ± 1 Ma, as given by fractions 1 and 3. The weighted mean $^{207}Pb–^{206}Pb$ age for all five fractions from this sample is 426 ± 2 Ma with a χ^2 value of 2.4.

Fraction 2, consisting of a single zircon needle, yields a considerably older $^{206}Pb–^{238}U$ date of 462 ± 1 Ma relative to the other four fractions. Although it yields a $^{207}Pb–^{206}Pb$ age consistent with the other fractions, fraction 2 is 9.1% reversely discordant, having significantly older apparent Pb–U ages. The reason for this is unclear. There is no morphological evidence for an inherited zircon component in zircon from this rock, nor do any of the other zircon fractions show any isotopic evidence for inheritance. In addition, a mixture of inherited zircon with an igneous component of Silurian age would be expected to produce normal discordance and shift the $^{207}Pb–^{206}Pb$ age to older values, in contrast to what is observed. A possible explanation for the observed reverse discordance of fraction 2 is incomplete dissolution of the zircon during which lead was fractionated from uranium.

93-B-3A, monzodiorite

This sample comes from the interior of the Ballachulish Igneous Complex, *c*. 1 km south of the summit of Sgorr Dhonuill (Fig. 1). The rock consists of a matrix of plagioclase and minor K-feldspar, with phenocrysts of clinopyroxene, orthopyroxene and minor biotite, and accessory ilmenite, iron oxides, apatite, zircon and monazite.

Zircons from this rock are morphologically distinct from those seen in the appinite sample described above. A large proportion of the zircons retrieved from 93-B-3A are fragments of larger grains, presumably fractured during sample crushing and milling. Grain shapes are generally equant rather than elongate, and the zircon is clear and colourless.

Four zircon fractions were analysed, three of these consisting of multiple grains, the other being a single zircon fragment. Two of the multi-grain fractions were abraded before analysis. Results from fractions 2, 3 and 4 are within uncertainty of concordia at the 2σ level and yield consistent $^{206}Pb–^{238}U$ ages with a weighted mean of 423.6 ± 0.5 Ma and a χ^2 value of 0.5 (Fig. 2b). Fraction 1 is slightly discordant and yields a younger $^{206}Pb–^{238}U$ age of 419 ± 1 Ma suggestive of minor Pb loss. Alternatively, if $^{207}Pb–^{206}Pb$ ages are preferred over $^{206}Pb–^{238}U$ ages, the weighted mean of all four fractions is 427 ± 1 Ma with a χ^2 value of 1.7.

93-B-6, granite

This sample comes from the margins of the granite that makes up the central part of the Ballachulish Igneous Complex, and

Table 1. *U–Pb TIMS analyses for Ballachulish Igneous Complex, Glencoe Volcanic Complex and Ballachulish metamorphic aureole*

Sample description	Weight (μg)	U (ppm)	Th (ppm)	Pb (ppm)	Th/U	TCPb (pg)	$^{207}Pb/^{206}Pb$	$^{206}Pb/^{238}U$	$^{207}Pb/^{235}U$	$^{207}Pb/^{206}Pb$	$^{206}Pb/^{238}U$	$^{207}Pb/^{235}U$	$^{207}Pb/^{206}Pb$	%Disc.
BALLACHULISH IGNEOUS COMPLEX														
Appinite 93-B-20														
1, 5 clear, elong. needles zircon, nabr.	11	210	276	21	1.32	30	351	0.0677 ± 2	0.517 ± 3	0.0554 ± 3	422 ± 0.9	423 ± 2	427 ± 11	1.1
2, single clear needle zircon, nabr.	8	222	276	24	1.25	28	309	0.0744 ± 2	0.567 ± 3	0.0553 ± 3	462 ± 1	456 ± 2	425 ± 12	−9.1
3, 7 stubby zircons, nabr.	20	51	69	5	1.36	16	292	0.0676 ± 2	0.515 ± 3	0.0552 ± 3	422 ± 0.9	422 ± 2	422 ± 14	0.07
4, 14 clear, elong. needles zircon, nabr.	19	564	457	44	0.81	29	1550	0.0671 ± 2	0.510 ± 1	0.0552 ± 1	418 ± 0.9	419 ± 0.9	420 ± 3	0.3
5, 25 clear, elong. needles zircon, nabr.	16	337	395	29	1.17	11	2039	0.0673 ± 2	0.515 ± 2	0.0555 ± 1	420 ± 1	422 ± 1	433 ± 3	3.1
Monzodiorite 93-B-3A														
1, 10 zircon fragments, nabr.	82	418	399	33	0.96	28	5140	0.0672 ± 2	0.513 ± 2	0.0554 ± 0.4	419 ± 1	421 ± 1	429 ± 2	2.3
2, single zircon fragment, nabr.	10	407	404	36	0.99	29	589	0.0679 ± 1	0.518 ± 2	0.0554 ± 2	423 ± 0.8	424 ± 1	427 ± 6	0.9
3, 12 clear, fragments, zircon, abr.	66	331	315	27	0.95	31	2984	0.0679 ± 1	0.519 ± 1	0.0554 ± 1	424 ± 0.9	424 ± 0.8	428 ± 2	1.0
4, 17 clear, fragments, zircon, abr.	66	227	210	18	0.93	26	2459	0.0680 ± 1	0.518 ± 1	0.0553 ± 1	424 ± 0.8	424 ± 0.8	423 ± 2	−0.2
Granite 93-B-6														
1, 13 clear, elong., euh. zircons, nabr.	29	197	118	15	0.60	28	876	0.0675 ± 1	0.517 ± 2	0.0555 ± 1	421 ± 0.8	423 ± 1	434 ± 5	3.1
2, 8 clear, stubby, euh. zircons, nabr.	8	459	250	45	0.60	69	257	0.0737 ± 3	0.595 ± 5	0.0586 ± 4	458 ± 2	474 ± 3	550 ± 15	17.3
3, 11 clear, elong., euh. zircons, abr.	48	139	104	11	0.75	22	1281	0.0674 ± 3	0.517 ± 3	0.0557 ± 2	421 ± 2	423 ± 2	439 ± 7	4.3
4, 10 clear, elong., euh. zircons, abr.	18	123	72	10	0.59	2	5229	0.0759 ± 1	0.645 ± 2	0.0616 ± 1	472 ± 0.9	505 ± 1	661 ± 3	29.7
GLENCOE VOLCANIC COMPLEX														
Rhyolite gf-99-34														
1, 9 clear, euh. zircons, nabr.	39	126	53	18	0.42	5	7818	0.1323 ± 2	1.494 ± 3	0.0819 ± 1	801 ± 1	928 ± 1	1243 ± 1	37.8
2, 8 clear, elong., euh. zircon, nabr.	33	62	48	5	0.76	8	1214	0.0739 ± 2	0.627 ± 2	0.0615 ± 1	460 ± 1	494 ± 1	656 ± 5	31.0
3, single, clear fragment, zircon, nabr.	26	125	100	10	0.81	6	2218	0.0663 ± 1	0.510 ± 2	0.0558 ± 1	414 ± 0.9	418 ± 1	444 ± 6	7.0
4, 24 clear, elong., euh. zircon, nabr.	21	220	181	18	0.82	14	1429	0.0700 ± 1	0.562 ± 1	0.0582 ± 1	436 ± 0.8	453 ± 0.9	537 ± 3	19.4
5, 20 clear, elong., euh. zircon, nabr.	13	217	164	18	0.75	48	229	0.0588 ± 13	0.467 ± 14	0.0577 ± 11	368 ± 8	389 ± 10	518 ± 42	29.7
6, 9 clear, elong., euh. zircon, nabr.	6	157	156	12	0.99	5	737	0.0618 ± 1	0.473 ± 3	0.0554 ± 3	387 ± 0.7	393 ± 2	430 ± 11	10.3
Andesite gf-99-40														
1, 2 clear, elong., euh. zircon, nabr.	7	191	93	13	0.49	4	1265	0.0639 ± 3	0.483 ± 3	0.0548 ± 2	399 ± 2	400 ± 2	406 ± 8	1.6
2, 6 rounded, eqnt, zircon, nabr.	16	211	37	29	0.18	17	1678	0.1358 ± 3	1.379 ± 3	0.0737 ± 1	821 ± 1	880 ± 1	1032 ± 2	21.8
3, 2 clear, euh. zircon, nabr.	12	61	58	5	0.95	6	539	0.0636 ± 1	0.487 ± 3	0.0555 ± 3	397 ± 0.8	403 ± 2	434 ± 14	8.7
BALLACHULISH METAMORPHIC AUREOLE														
Migmatite gf-99-128														
Granodiorite component Gd														
2, 15 rounded, eqnt, zircon, nabr.	55	158	57	27	0.36	8	10891	0.1668 ± 4	1.780 ± 4	0.0774 ± 1	994 ± 2	1038 ± 2	1130 ± 1	13.1
3, 30 elong., euh. zircon, nabr.	59	149	53	26	0.36	13	6936	0.1651 ± 3	1.886 ± 4	0.0829 ± 1	985 ± 2	1076 ± 2	1266 ± 1	24.0
Pelitic component A1														
1, 20 elong., euh. zircon, nabr.	10	204	58	35	0.29	39	521	0.1549 ± 10	1.738 ± 11	0.0814 ± 3	928 ± 6	1023 ± 4	1230 ± 9	26.3
Kspar-bearing ductile component B														
1, 60 clear, euh. zircon, nabr.	26	98	31	16	0.32	5	4807	0.1622 ± 3	1.693 ± 4	0.0757 ± 1	969 ± 2	1006 ± 1	1088 ± 2	11.7
2, 50 trans., eqnt., rounded, zircon, nabr.	16	215	70	40	0.33	7	6067	0.1830 ± 3	2.131 ± 4	0.0844 ± 1	1084 ± 2	1159 ± 1	1302 ± 1	18.2
Migmatite 92-B-43B														
1, 6 euh. elong., zircon, nabr.	11	42	12	6	0.27	4	895	0.1334 ± 3	1.335 ± 6	0.0725 ± 3	808 ± 2	861 ± 3	1001 ± 7	20.5
Metacarbonate gf-99-63														
1, 11 very tiny, baddeleyite	3	150	6	12	0.04	9	219	0.0684 ± 5	0.535 ± 8	0.0568 ± 8	426 ± 3	435 ± 5	484 ± 29	12.4
2, 52 trans., s. tan, no vis. core baddeleyite	8	183	10	12	0.06	4	1551	0.0673 ± 2	0.513 ± 2	0.0553 ± 2	420 ± 1	420 ± 1	423 ± 6	0.6
3, 22 with brn. core regions baddeleyite	3	187	3	12	0.01	4	662	0.0676 ± 1	0.511 ± 4	0.0548 ± 4	422 ± 1	419 ± 3	403 ± 16	−4.8

vis., visible; trans., transparent; s., slightly; brn., brown; elong., elongate; eqnt., equant; euh., euhedral; abr., abraded; nabr., non-abraded.

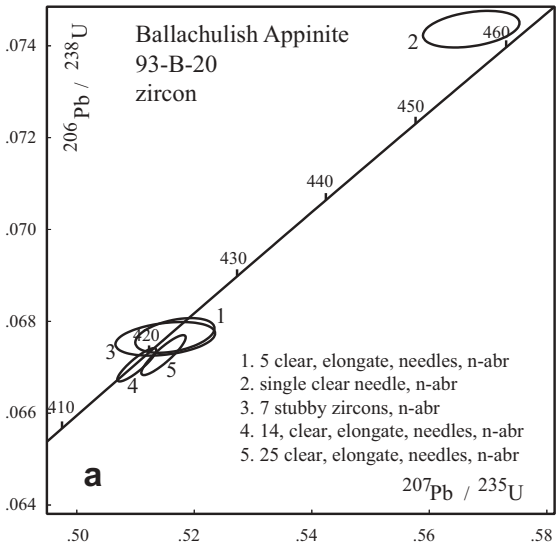

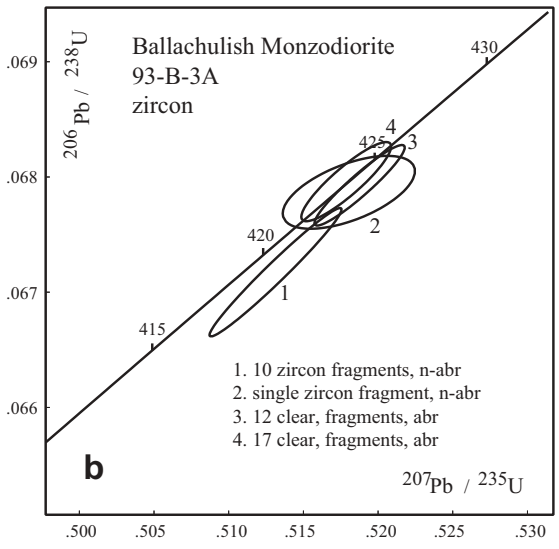

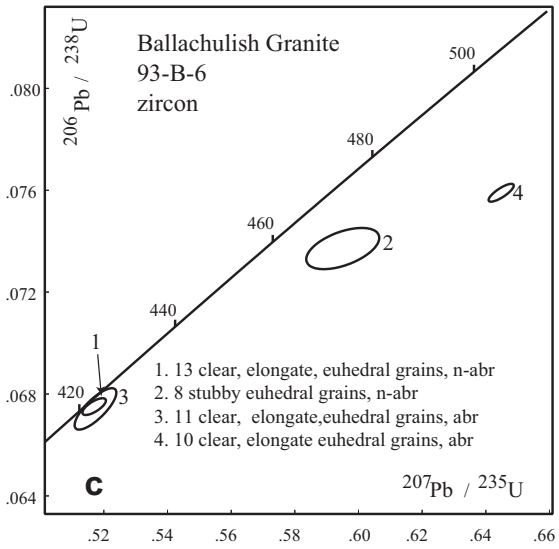

Fig. 2. U–Pb concordia diagrams for zircon analyses from the Ballachulish Igneous Complex. Zircon was separated from one sample for each of three rock types, with each analysis representing a different zircon fraction from the same sample. n-abr, non-abraded; abr, abraded. (**a**) Ballachulish Igneous Complex appinite; (**b**) Ballachulish Igneous Complex monzodiorite; (**c**) Ballachulish Igneous Complex granite.

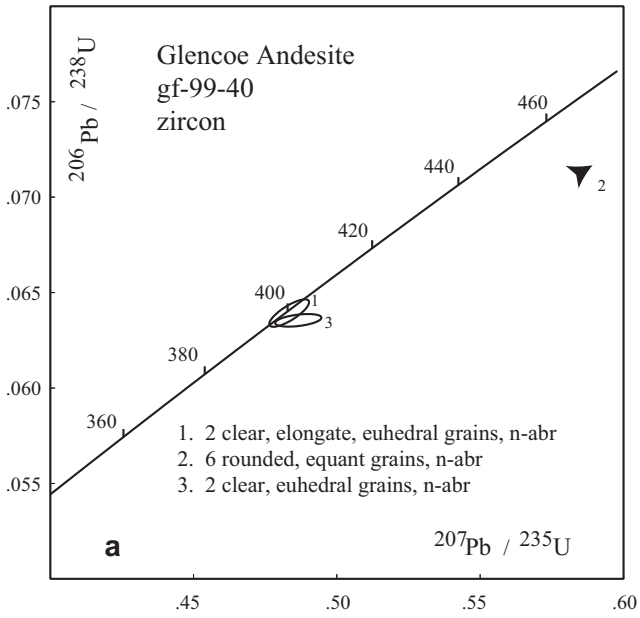

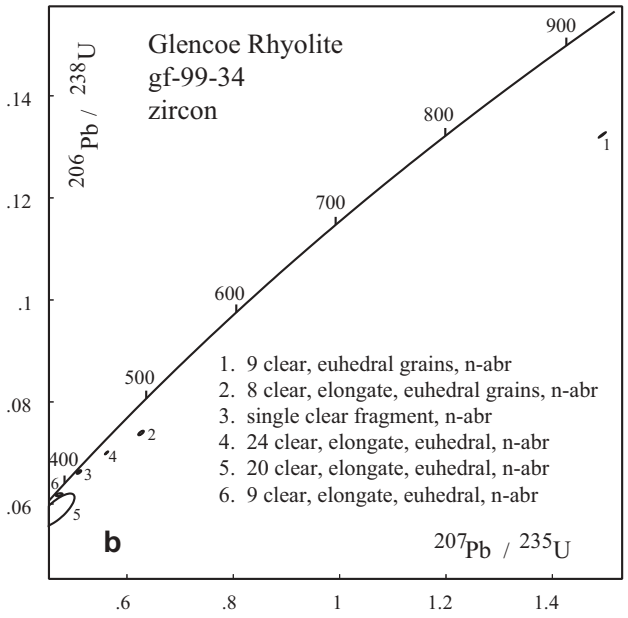

Fig. 3. U–Pb concordia diagrams for zircon analyses from the Glencoe Volcanic Complex. Several different zircon fractions were analysed from each of an andesite and rhyolite sample. n-abr, non-abraded; abr, abraded. (**a**) Glencoe Volcanic Complex andesite; (**b**) Glencoe Volcanic Complex rhyolite.

was collected a few hundred metres west of Sgorr Dhonuill (Fig. 1). The rock consists of plagioclase, K-feldspar, quartz, clinopyroxene and biotite, with abundant apatite, and ilmenite. Zircon is relatively abundant and occurs as euhedral, slightly elongate (aspect ratio typically *c*. 3) grains with well-formed crystal faces and pointed terminations. Backscattered electron (BSE) and cathodoluminescence imaging reveals concentric internal zonation in the outer parts of most crystals, and in some grains the presence of a compositionally distinct core.

Four zircon fractions have been analysed, two of which were abraded before analysis (Fig. 2c). Fractions 2 and 4 are markedly discordant and yield $^{207}Pb–^{206}Pb$ ages of 550 and 661 Ma, respectively, indicating the presence of a significant inherited component in these grains. Fractions 1 and 3 plot close to concordia, although slightly discordant, and yield consistent $^{206}Pb–^{238}U$ ages of 421 ± 1 Ma.

Discussion of ages from the Ballachulish Igneous Complex

Despite a considerable amount of relatively concordant data, it is not straightforward to make a best estimate for the age from this group of data. This is due to small departures from concordia introducing relatively large differences between $^{206}Pb–^{238}U$ and $^{207}Pb–^{206}Pb$ ages, a problem common to U–Pb ages from the Phanerozoic part of the time scale. This raises the issue of whether to place more confidence in $^{206}Pb–^{238}U$ ages or $^{207}Pb–^{206}Pb$ ages. Arguments can be made in favour of either age type. The $^{206}Pb–^{238}U$ ages are relatively precise, but are susceptible to minor Pb loss, which is very difficult to identify in this part of the concordia curve. The $^{207}Pb–^{206}Pb$ ages are less susceptible to Pb loss particularly if any Pb loss was recent, but are less precise than the $^{206}Pb–^{238}U$ ages as a result of the small amounts of measured ^{207}Pb. In addition, $^{207}Pb–^{206}Pb$ ages are relatively sensitive to the choice of initial Pb isotopic composition, and are also more susceptible to uncertainties in the U decay constants, which expand the concordia curve from a line to a band. For zircons showing no evidence for inheritance, such as those in the Ballachulish appinite and monzodiorite, the oldest near-concordant $^{206}Pb–^{238}U$ ages are likely to be the most reliable of the $^{206}Pb–^{238}U$ ages, having experienced the least Pb loss. This approach yields best estimates of 422 ± 1 Ma, and 424 ± 1 Ma for the appinite and monzodiorite, respectively. These $^{206}Pb–^{238}U$ ages represent minimum estimates if minor Pb loss has occurred. In contrast, where inheritance is clearly present, such as for the Ballachulish granite, the effects of inheritance and Pb loss compete, making rigorous evaluation of the $^{206}Pb–^{238}U$ ages very difficult. It is therefore not clear whether the most concordant zircon fractions from the granite, with $^{206}Pb–^{238}U$ ages of 421 Ma, should be regarded as maximum or minimum ages, although comparison with results from the other two Ballachulish Igneous Complex samples suggests these are likely minimum estimates.

In the appinite and monzodiorite samples, where inheritance appears to be absent, the $^{207}Pb–^{206}Pb$ ages, being less susceptible to Pb loss, give a more robust age estimate, albeit with reduced precision. The appinite and monzodiorite yield $^{207}Pb–^{206}Pb$ best estimates of 426 ± 2 Ma, and 427 ± 1 Ma, respectively. Where inheritance is demonstrably present, as in the case of the granite, the $^{207}Pb–^{206}Pb$ ages do not give a reliable age estimate, and we are restricted to using the most concordant $^{206}Pb–^{238}U$ ages.

Comparison of results from the three samples from the Ballachulish Igneous Complex suggests that, at the level of precision available with the current data, there is no significant difference in age between samples. We have therefore pooled the most reliable results from all three samples. Fractions 1 and 3 from the appinite, fractions 2, 3 and 4 from the monzodiorite and fractions 1 and 3 from the granite yield a weighted mean $^{206}Pb–^{238}U$ age of 423 ± 0.3 Ma with a χ^2 value of 1.9. All nine fractions from the appinite and monzodiorite yield a weighted mean $^{207}Pb–^{206}Pb$ age of 427 ± 1 Ma, with a χ^2 value of 1.8. We see no *a priori* reason for preferring $^{206}Pb–^{238}U$ v. $^{207}Pb–^{206}Pb$ ages or vice versa. To aid comparison with $^{207}Pb–^{206}Pb$ ages reported for other igneous rocks of the Argyll Region (Rogers & Dunning 1991; Stewart *et al*. 2001) we take the $^{207}Pb–^{206}Pb$ age of 427 ± 1 Ma as the best estimate for age of the Ballachulish Igneous Complex, although noting that the $^{206}Pb–^{238}U$ age is slightly younger at 423 ± 0.3 Ma.

Results presented above indicate that magmatism within the Ballachulish Igneous Complex lasted no more than a few million years, and probably considerably less. This is consistent with geological evidence of gradational contacts between appinitic and dioritic magmas, and dioritic and granitic magmas, suggesting that each successive magmatic phase was intruded while the previous phase was still at least partly molten (Troll & Weiss 1991). A short-lived duration of magmatism, as suggested by indistinguishable ages from different phases of the complex, is also consistent with results of thermal modelling, which match the temperature conditions reconstructed from the thermal aureole by assuming essentially instantaneous emplacement of the Ballachulish Igneous Complex at temperatures of *c*. 1100 °C (Buntebarth 1991).

The $^{207}Pb–^{206}Pb$ age of 427 ± 1 Ma presented here for the Ballachulish Igneous Complex is very similar to those reported by Rogers & Dunning (1991) for appinites at Rubha Mor (427 ± 3 Ma; $^{206}Pb–^{238}U$ titanite), a few kilometres west of the Ballachulish Igneous Complex, and at Garabal Hill (429 ± 2 Ma; $^{207}Pb–^{206}Pb$ zircon) and Arrochar (426 ± 3 Ma; $^{206}Pb–^{238}U$ titanite), *c*. 50 km to the south. This age is also indistinguishable from $^{207}Pb–^{206}Pb$ zircon ages reported from the Strontian Granodiorite (425 ± 3 Ma; Rogers & Dunning 1991) and the Clunes Tonalite (428 ± 2 Ma; Stewart *et al*. 2001) in the Argyll Region. Taken together, these data present a picture of relatively widespread appinite-related intrusive activity occurring essentially synchronously across the Argyll Region between about 425 and 428 Ma, and possibly related to transcurrent movement along the Great Glen Fault and related structures (Jacques & Reavy 1994; Stewart *et al*. 2001).

Results from the Glencoe Volcanic Complex

gf-99-40, andesite

This sample was collected from the lowermost cliff exposures SSW of the Achnambeithach mountain rescue post (south of Loch Achtriochtan) near the western entrance to Glencoe (Fig. 1). The sample is an amygdaloidal andesite flow from Group I of Bailey & Maufe (1960) and is cut by steeply dipping rhyolite dykes, trending N40°E, which probably represent feeders of the overlying rhyolite (gf-99-34). Zircon is rare in this rock, and relatively few grains were retrieved from the mineral separation procedure, allowing for only three fractions to be analysed (Fig. 3a). Morphologically zircon falls into two groups. Fractions 1 and 3 consist of euhedral, slightly elongate (aspect ratios *c*. 2.5) clear grains with pointed terminations. Fraction 2 consists of rounded, relatively equant, anhedral grains. Fraction 2 is very discordant with a $^{207}Pb–^{206}Pb$ age of 1032 Ma, clearly indicating the presence of an inherited component. Fractions 1 and 3 are near concordant and yield consistent $^{206}Pb–^{238}U$ ages of

399 ± 2 Ma and 397 ± 1 Ma, respectively. Although we cannot rule out the possibility of minor Pb loss having affected these grains, the consistency between the two fractions lends some confidence to these ages representing the time of zircon crystallization and presumably the time of andesite emplacement. Alternatively, if $^{207}Pb–^{206}Pb$ ages are preferred, the best estimate comes from the most concordant analysis, fraction 1, giving 406 ± 8 Ma.

gf-99-34, rhyolite

This sample comes from *c*. 50 m west of the 'Queen's Cairn', on the northern side of the road through the Pass of Glencoe (Fig. 1). In outcrop the rhyolite has a brecciated appearance, with finely layered fragments of centimetre to tens of centimetre size randomly oriented in a fine-grained matrix. Feldspar phenocrysts occur both in layered fragments and in the matrix. This texture is interpreted as the result of early crystallized, flow-banded rhyolite having been ripped up and reoriented by subsequent extrusion events. This rhyolite comes from Group II in the Glencoe volcanosedimentary sequence of Bailey & Maufe (1960).

Zircon is abundant and occurs primarily as clear, elongate grains with aspect ratios of *c*. 4. Commonly these elongate grains contain an inclusion-rich, rod-shaped core. A secondary zircon population occurs as less elongate (aspect ratios of 2–3) subhedral grains with rounded terminations. Six zircon fractions were analysed from this sample and all show evidence of inheritance and/or Pb loss, making age determination problematic (Fig. 3b). Fractions 1, 2, 3 and 4 all show considerable inheritance and define a relatively well-defined discordia line. Of these, fraction 3 lies closest to concordia and has a $^{206}Pb–^{238}U$ age of 414 ± 1 Ma but is still 7% discordant and probably contains some inheritance. The discordia defined by these four fractions has an upper intercept of 1531 ± 22 Ma and a lower intercept of 407 ± 9 Ma, with a χ^2 value of 0.8 (mean square weighted deviation). This lower intercept lies within error of the near-concordant $^{206}Pb–^{238}U$ ages from the andesite described above (gf-99-40), and is also very close to the $^{207}Pb–^{206}Pb$ age of the most concordant andesite zircon fraction (406 ± 8 Ma). Fractions 5 and 6 are also discordant but lie below the discordia trend defined by the other four fractions, and appear to have been variably affected by post-crystallization Pb loss.

Discussion of ages from the Glencoe Volcanic Complex

Given the presence of an inherited component in zircon from the rhyolite sample, as well as possible minor Pb loss in the andesite, interpretation of the Glencoe age data is subject to larger uncertainties than for the Ballachulish Igneous Complex. The consistency of $^{206}Pb–^{238}U$ ages for two near-concordant analyses from the andesite sample suggests a best estimate of 397 ± 1 Ma, although we cannot rule out minor Pb loss having affected these analyses. If $^{207}Pb–^{206}Pb$ ages are preferred over $^{206}Pb–^{238}U$ ages, the best estimates come from the lower intercept of the discordia line defined by the rhyolite analyses (407 ± 9 Ma) and the $^{207}Pb–^{206}Pb$ age of the most concordant andesite analysis (406 ± 8 Ma). These data combined yield a weighted mean $^{207}Pb–^{206}Pb$ age of 406 ± 6 for the Glencoe Volcanic Complex.

Thus, even though the Glencoe Volcanic Complex has been grouped together with the Ballachulish Igneous Complex and other *c*. 425 Ma intrusive complexes as part of the Argyll Suite (Stephenson & Gould 1995), the volcanic activity at Glencoe as well as the cross-cutting Cruachan Granite of the Etive Complex appear to post-date these intrusive complexes by *c*. 20 Ma.

Relationship between the Ballachulish Igneous Complex and Glencoe Volcanic Complex

Comparison of U–Pb results from the Ballachulish Igneous Complex and Glencoe Volcanic Complex suggests that, irrespective of whether $^{206}Pb–^{238}U$ or $^{207}Pb–^{206}Pb$ ages are preferred, intrusion of the Ballachulish Igneous Complex occurred 20–25 Ma earlier than extrusion of the Glencoe Volcanic Complex. This result, in combination with geological features of the Ballachulish Igneous Complex and Glencoe Volcanic Complex, places constraints on the exhumation history of this part of the Dalradian sequence in the Argyll region.

Various lines of petrological evidence indicate emplacement pressure of 3.0 ± 0.5 kbar for the Ballachulish Igneous Complex, corresponding to a depth of emplacement of 10 ± 2 km (Pattison 1989, 1992; Pattison & Harte 1997). In contrast, the volcanic succession of the Glencoe Volcanic Complex, containing lava flows, unconformities and sedimentary horizons, was clearly emplaced at the Earth's surface. This difference in emplacement depth of *c*. 10 km between the Ballachulish Igneous Complex and Glencoe Volcanic Complex, together with the relative age difference of *c*. 20 Ma, yields an average exhumation rate of *c*. 0.5 km Ma^{-1} for the region around the Ballachulish Igneous Complex over the period between Ballachulish Igneous Complex emplacement and Glencoe Volcanic Complex extrusion.

Several qualifying considerations are necessary in evaluating the reliability of this estimate. The calculation assumes that the Ballachulish Igneous Complex and the region immediately surrounding it was at, or very close to, the Earth's surface at the time the Glencoe Volcanic Complex was active. This implies block uplift of the Argyll region without significant relative vertical displacements between the Glencoe Volcanic Complex and Ballachulish Igneous Complex regions since Glencoe Volcanic Complex magmatic activity. Such vertical displacements could potentially be accommodated either along folds or faults separating the two regions, or via tilting of the entire region to bring the Ballachulish Igneous Complex to the present-day exposure level alongside the Glencoe Volcanic Complex.

Block tilting subsequent to extrusion of the Glencoe Volcanic Complex is not supported by the fact that the Glencoe volcanic rocks are still essentially flat lying. Similarly, the broadly contemporaneous Lorne Lavas, which crop out *c*. 15 km south of the Ballachulish Complex, are also essentially flat lying. Droop & Treloar (1981) have estimated a maximum of 3 km of tilt over 35 km in the Etive Complex 8 km SE of Ballachulish. A similar magnitude of tilt between Ballachulish and Glencoe (a distance of *c*. 10 km) could account for less than 1 km of vertical displacement, clearly not sufficient to account for the preserved *c*. 10 km difference in depth of palaeomagmatic activity at the current exposure surface.

Movement along the Glencoe Ring Fault is the most likely site of significant vertical movement between the Glencoe Volcanic Complex and the Ballachulish Igneous Complex synchronous with or subsequent to Glencoe volcanic activity. The magnitude of caldera subsidence at Glencoe must be subtracted from the apparent 10 km difference in structural level between the Ballachulish Igneous Complex and Glencoe Volcanic Complex to make an accurate estimate of exhumation rate in the period between Ballachulish Igneous Complex and Glencoe Volcanic Complex igneous activity. The detailed volcanic reconstruction of Moore & Kokelaar (1998) suggests *c*. 1 km of downthrow on

the Ring Fault in the SW of the Glencoe Volcanic Complex, with an additional, earlier history involving >700 m of incremental subsidence within the caldera, giving an overall estimate of the order of 2 km of subsidence. This leaves *c*. 8 km exhumation of the Ballachulish Igneous Complex prior to Glencoe Volcanic Complex activity. Further indirect evidence for exhumation of the entire Argyll region prior to Glencoe Volcanic Complex activity is provided by the existence of boulders of Rannoch Moor Granite within conglomerates in the Glencoe graben (Taubeneck 1967; Moore & Kokelaar 1998), indicating that the region immediately east of the Glencoe Volcanic Complex had experienced sufficient exhumation prior to volcanic activity to expose the Rannoch Moor Granite. However, no sufficiently precise estimates exist for the age or depth of emplacement of the Rannoch Moor Granite to provide a quantitative estimate of exhumation rate east of the Glencoe Volcanic Complex.

The evidence presented above suggests that structural movement subsequent to the Glencoe Volcanic Complex cannot account for the difference in depth of magmatic activity, leaving the most likely explanation that the Ballachulish Igneous Complex and its immediate surrounds were exhumed from 10 km to within *c*. 2 km of the Earth's surface by the time of Glencoe volcanic activity, giving an average exhumation rate of 0.4 km Ma^{-1} for the period *c*. 425–405 Ma. This estimate is very similar to the value of 0.5 km Ma^{-1} presented by Dempster (1985) for exhumation in the eastern Grampians over the period 410–390 Ma.

Regional context

A combination of existing precise age constraints (Rogers & Dunning 1991; Stewart *et al*. 2001) with the new data for the Ballachulish Igneous Complex and Glencoe Volcanic Complex suggests two distinct, short-lived periods of late Caledonian magmatism in Scotland, separated by about 20 Ma. The first, characterized by appinites and related plutons, occurred at *c*. 425–428 Ma. The second, represented by the Glencoe Volcanic Complex, Etive Complex and cross-cutting Etive dykes, occurred at *c*. 400–405 Ma. Resolution of these two distinct episodes of magmatic activity, based on improved precision in age constraints, contrasts with the range of ages apparent in older, lower precision datasets (e.g.Thirlwall 1988; Stephenson & Gould 1995). Further geochronology on igneous bodies in the Argyll region will be required to clarify this emerging trend. For example, geological similarities between the Glencoe Volcanic Complex and the Ben Nevis Complex, *c*. 10 km to the north, suggest that the Ben Nevis Complex may be of a similar age. Of particular interest would be a precise age for the Etive dykes, which appear to represent the final stage of late Caledonian magmatic activity, and an age for the Rannoch Moor Granite, cobbles of which occur in conglomerates at the base of the Glencoe volcanosedimentary sequence (Moore & Kokelaar 1998).

Baddeleyite, zircon and monazite paragenesis in the Ballachulish metamorphic aureole

Having determined the age of the Ballachulish Igneous Complex, we now examine the behaviour of the U-bearing accessory minerals baddeleyite, zircon and monazite in the Ballachulish metamorphic aureole. Baddeleyite is commonly used to date mafic rocks (e.g. Heaman & LeCheminant 1993), but we show below that it can also record the age of metamorphism in upper amphibolite-facies carbonate rocks. Zircon and monazite are the two most commonly used minerals for U–Pb dating of tectonometamorphic events. The conventional paradigm is that because monazite has a lower U–Pb closure temperature than zircon, it will typically record a somewhat younger age than zircon in metamorphic rocks. This expectation implicitly assumes that monazite records a closure age, and that zircon grows before monazite closes during metamorphism. However, apart from high-*T* granulite-facies rocks, the majority of metamorphic rocks never experience temperatures in excess of the monazite closure temperature (750–800 °C, Smith & Giletti 1997; Cherniak *et al*. 2000). Consequently, U–Pb ages measured on both metamorphic zircon and monazite are typically growth (or recrystallization) ages rather than closure ages, and thus the interpretation of metamorphic zircon and monazite ages is critically dependent on an understanding of the physical and chemical conditions of mineral growth (or recrystallization). Despite recent advances in this field (Fraser *et al*. 1997; Pyle & Spear 1999; Degeling *et al*. 2001; Rubatto *et al*. 2001; Williams 2001), the controls on metamorphic growth of zircon and monazite remain relatively poorly understood. In an effort to tackle this problem we have investigated the response of zircon and monazite in the well-constrained metamorphic setting of the Ballachulish aureole.

The Ballachulish metamorphic aureole

The Ballachulish aureole is one of the world's most thoroughly documented examples of contact metamorphism (Pattison & Harte 1997, and references therein). A variety of sedimentary lithologies have been metamorphosed including pelites, psammites, quartzites and carbonates. These host rocks are part of the Dalradian sedimentary package, and were subjected to regional Caledonian metamorphism between *c*. 520 and 490 Ma (Dempster 1985), some 70 Ma prior to intrusion of the Ballachulish Igneous Complex. Regional metamorphic grade varies in the Ballachulish region from chlorite grade in the NW to garnet grade in the SE, with estimated *P*–*T* conditions ranging from *c*. 450 to *c*. 550 °C from NW to SE, at *c*. 6 kbar (Pattison & Voll 1991). By the time of intrusion of the Ballachulish Igneous Complex at *c*. 427 Ma, regional *P*–*T* conditions are estimated to have dropped to 250–300 °C at around 3 kbar. The metamorphic aureole varies in width from *c*. 400 to 1700 m, based on first occurrence of cordierite in metapelites, and ranges in grade from ambient regional conditions up to migmatite grade and locally low-pressure granulite grade immediately adjacent to the igneous contacts.

Baddeleyite in the Ballachulish aureole

Baddeleyite (ZrO_2) is increasingly used for U–Pb geochronology, having the desirable characteristics of sufficient U content, very little initial common Pb, and high retentivity of radiogenic Pb (Heaman & LeCheminant 1993). The most common application of baddeleyite in geochronology is in dating mafic dykes (e.g. Heaman & Tarney 1989; LeCheminant & Heaman 1989; Wingate *et al*. 2000); however, baddeleyite has also been reported from metacarbonate rocks (Purtscheller & Tessadri 1985; Kato & Matsubara 1991). In a detailed study of accessory minerals in the siliceous dolomites of the Ballachulish aureole, Ferry (1996a) documented the presence of baddeleyite in the highest-grade part of the aureole, and proposed a baddeleyite isograd based on the reaction

$$\text{zircon} + 2\text{dolomite} = \text{baddeleyite} + \text{forsterite} + 2\text{calcite} + 2CO_2.$$

This is the same reaction as proposed by Kato & Matsubara

(1991). Ferry (1996a) estimated the conditions of the baddeleyite isograd to be 660–710 °C and X_{CO2} of 0.76–0.95, at a pressure of 3 kbar. The proposal of this isograd reaction predicts that baddeleyite in the Ballachulish metacarbonates is of contact metamorphic origin, and thus should record the same age as the Ballachulish Igneous Complex. To test this prediction we have dated baddeleyite from the Ballachulish carbonates via the TIMS method described above.

U–Pb results; sample gf-99-63 (metacarbonate)

Sample gf-99-63 was collected from the inner part of the Ballachulish metamorphic aureole in the Allt Giubhsachain area on the eastern side of the Ballachulish Igneous Complex, where baddeleyite was described by Ferry (1996a). Baddeleyite was initially identified in thin section via the use of BSE imaging and energy dispersive X-ray spectra. Grains identified in thin section were typically <50 μm in long dimension, and commonly <20 μm (Fig. 4). As baddeleyite has a platy mineral habit, it was feared that grains might be lost on the Wilfley table during standard mineral separation procedures, and therefore a modified separation procedure was used. The whole–rock sample was initially crushed, and milled to a coarse powder. This carbonate powder was then dissolved in acetic acid over a period of 2 days, the acid was then decanted and the residual solid material treated with fresh acetic acid for an additional 2 days. This procedure resulted in dissolution of most of the carbonate material, leaving silicates, oxides and sulphides, which were washed, dried and then processed in standard manner using methylene iodide (density 3.3 g cm^{-3}) and a Frantz magnetic separator. Baddeleyite occurs together with pyrite and spinel. Baddeleyite retrieved from this procedure occurs as light tan, tabular grains, many containing a dusty brown core. Grain size was typically of the order of 40 μm × 30 μm × 10 m, with no grains retrieved larger than about 60 μm in longest dimension.

Three baddeleyite fractions were analysed for U–Pb isotopic composition, each being a multi-grain fraction (Table 1; Fig. 5). Given the small grain size, and the relatively low U content (150–200 ppm), large numbers of grains were required to yield reasonable analytical precision. This is illustrated by the relatively imprecise data from fraction 1, consisting of only 11 grains. The three fractions yield $^{206}Pb–^{238}U$ ages that are indistinguishable from one another at the 2σ level, with a weighted mean of 421 ± 1 Ma, and are also indistinguishable from the $^{206}Pb–^{238}U$ results from the Ballachulish Intrusive Complex reported above. Similarly, the $^{207}Pb–^{206}Pb$ ages, although significantly less precise, are within 2σ uncertainty of the $^{207}Pb–^{206}Pb$ age of 427 ± 1 Ma for the Ballachulish Igneous Complex. These results indicate that all the baddeleyite found in this metacarbonate is of contact metamorphic origin, with no evidence for any inherited component, consistent with the interpretation of Ferry (1996a).

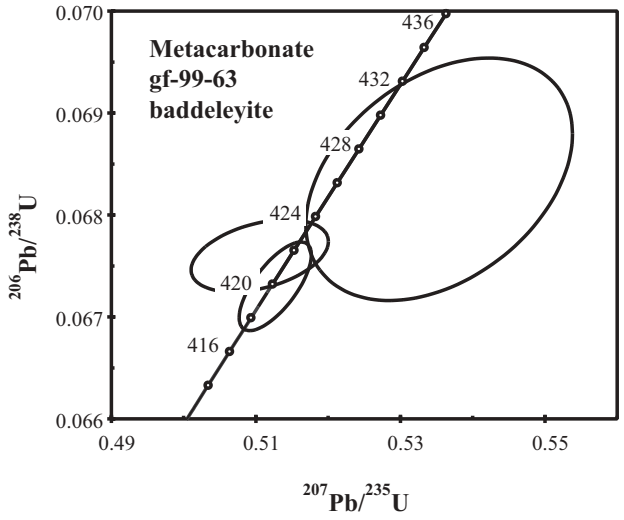

Fig. 5. U–Pb concordia diagram showing baddeleyite results from sample gf-99-63. Ellipses represent analyses of three separate baddeleyite fractions as shown in Table 1.

The U content of these metamorphic baddeleyites is towards the low end of the range seen in igneous baddeleyite, but not sufficiently different to be diagnostic. The Th/U ratios of the three baddeleyite fractions range from 0.01 to 0.06, not significantly different from Th/U values found in typical igneous baddeleyite (e.g. Heaman & LeCheminant 1993). As far as we are aware, these results are the first example of the use of baddeleyite to directly date metamorphism, and demonstrate a new tool for geochronology of high-grade metacarbonates, and perhaps other Si-poor metamorphic rocks.

Pelitic phase relations in the Ballachulish aureole

The distribution and texture of metamorphic zircon and monazite in metapelitic rocks has been investigated in a transect through the SW part of the Ballachulish aureole, near the peak of Fraochaidh (Fig. 6). Phase relations amongst pelitic rocks have been thoroughly documented (Pattison & Harte 1991, 1997) and five metamorphic zones defined. These are briefly summarized here to provide context for the zircon and monazite observations that follow.

Zone I. There are no obvious mineralogical effects attributable to contact metamorphism. Pelitic schists from this zone contain

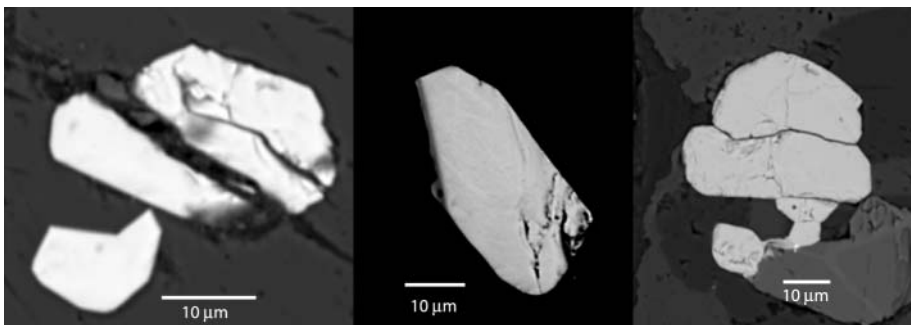

Fig. 4. BSE images of baddeleyite from metacarbonate sample gf-99-63.

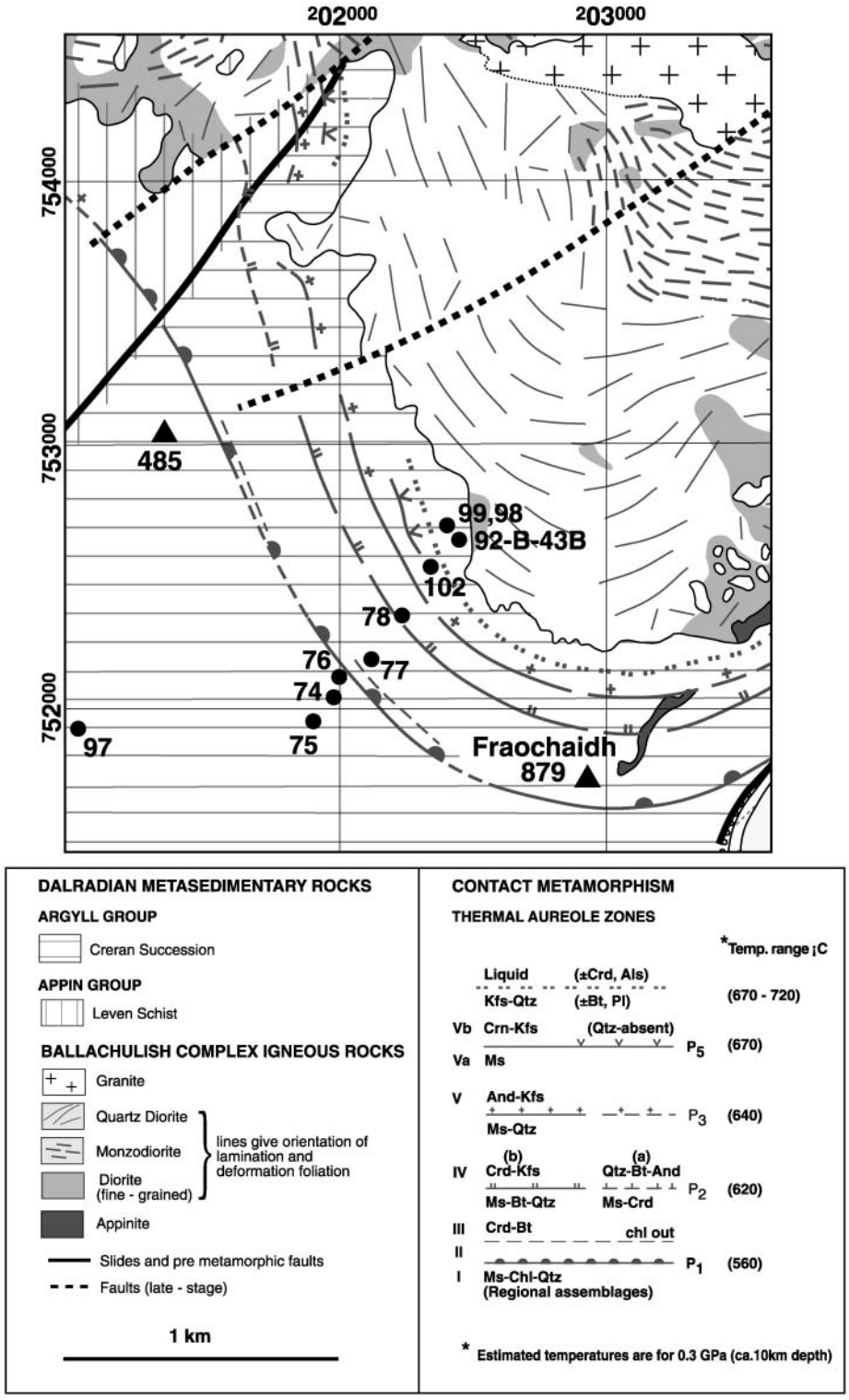

Fig. 6. Geological map showing sample localities in a transect through the Ballachulish metamorphic aureole in pelitic and semi-pelitic schists of the Creran succession, SW part of the thermal aureole as shown in Figure 1. All sample numbers are prefixed by gf-99- except for 93-B-43B. Grid numbers from National Grid Sheet NN 05/15. Base map from Pattison & Harte (2001).

mineral assemblages indicative of regional Caledonian metamorphism, typically consisting of Ms + Chl + Qtz ± Bt ± Grt, depending on bulk composition and position with respect to the regional garnet isograd.

Zone II. This zone is characterized by the first appearance of small circular or ellipsoidal spots of cordierite on cleavage surfaces. The production of cordierite is regarded to be the result of the reaction Ms + Chl + Qtz = Crd + Bt + H_2O (T 550–560 °C). In the SW part of the aureole this zone is very narrow.

Zone III. With increasing metamorphic grade, cordierite becomes larger and more abundant, chlorite is consumed leaving the assemblage Ms + Qtz + Bt + Crd, and the rocks become more massive via recrystallization. This is the widest metamorphic zone in the aureole.

Zone IV. This zone is marked by the incoming of K-feldspar, and the rocks take on a massive hornfels appearance. Muscovite is less abundant, and is absent from semi-pelitic layers. These mineralogical changes are accounted for by the reaction

$$Ms + Bt + Qtz = Kfs + Crd + H_2O (Tc.620\,^{\circ}C).$$

Zone V. This zone is defined by the coexistence of K-feldspar and andalusite, and the disappearance of either quartz or muscovite, depending on bulk composition, consistent with the reaction Ms + Qtz = And + Kfs + H_2O (*T c*. 640 °C).

Migmatites. In the upper part of Zone V, rocks take on a migmatitic appearance as a result of the presence of distinct K-feldspar + Qtz-rich leucosomes. Textural and structural analysis of these rocks strongly suggests local melt derivation (Pattison & Harte 1988; Harte *et al*. 1991). In the innermost part of the aureole, some samples show development of garnet, or garnet and hypersthene, indicative of low-pressure granulite-facies conditions and temperatures of 750–850 °C (Pattison 1989; Pattison & Harte 1997).

Zircon in the Ballachulish aureole

Outer Zone I

Sample gf-99-97, from the outer part of Zone I (Fig. 6), contains zircon that occurs commonly as broken fragments of larger grains (Fig. 7). Grain outlines appear to have been originally euhedral, but show evidence of some rounding and surface pitting. Internally, grains commonly show concentric compositional zonation, which is truncated at broken grain edges. These features are consistent with an igneous origin for these grains and subsequent physical transport during sedimentation, causing damage to crystal faces and in many cases fragmentation of original grains. These zircons from outside the metamorphic aureole are therefore interpreted as detrital grains incorporated in Dalradian sediments, and show no features that might be related to contact metamorphism.

Inner Zone I and Zones II and III

Zircons from the inner part of Zone I and up to Zone III (samples gf-99-75, 74, 116) commonly show irregular, embayed rims around a core that is similar in morphology to the detrital grains from the outermost part of the aureole (Fig. 7). The cores of these grains show no evidence for chemical dissolution, retaining a sharp, angular outline suggestive of a broken fragment of an originally euhedral grain. The narrow rims (generally *c*. 2–5 μm wide) on these grains therefore appear to be the result of precipitation of new zircon rather than partial recrystallization of detrital grains. The narrow zircon rims appear to have also been subject to dissolution, as evidenced by their discontinuous and deeply embayed morphology.

The presence of these rims of apparent new zircon growth at metamorphic grades corresponding to temperatures in the range *c*. 500–600 °C, significantly below partial melt conditions, is somewhat surprising. The studies of Rubatto *et al*. (2001) and Williams (2001), on regional low-pressure settings with similar rock types and range in metamorphic grade, both concluded that metamorphic zircon is not produced until partial melting occurs, and that detrital zircon is essentially unaffected at lower metamorphic grades. An exception to this general conclusion was reported by Rubatto *et al*. (2001) for samples from sillimanite–tourmaline-bearing veins regarded as the result of metamorphic fluid flow. Zircons from these samples were reported as euhedral and having a core–rim structure that was attributed to zircon growth in the presence of metamorphic fluid. Very high U contents (>5000 ppm) and corresponding extensive metamictization precluded sensitive high-resolution ion microprobe (SHRIMP) age determinations from these grains, and thus limited the geological interpretation of Rubatto *et al*. (2001).

The zircon rims seen in the lower-grade parts of the Ballachulish aureole do not come from vein-related samples. Petrological and stable isotopic evidence from the Ballachulish aureole suggests little exotic fluid infiltration during contact metamorphism (Hoernes *et al*. 1991; Ferry 1996b; Pattison & Harte 1997), so that an appeal to externally derived fluids to account for low-grade zircon growth seems unjustified. However, the occurrence of these zircon rims does coincide with the onset of dehydration reactions involving chlorite breakdown, which liberated significant volumes of hydrous fluid. Movement of such hydrous fluid vertically or laterally away from the aureole may potentially have led to precipitation of zircon rims on existing grains, although a source of Zr remains problematic, as we see no particular evidence for dissolution of pre-existing detrital grains in any part of the aureole.

Pelitic rocks in the Ballachulish aureole have also been subject to retrograde metamorphic fluid infiltration as revealed by extensive pinitization of cordierite, and local sericitic alteration of K-feldspar and chloritization of biotite. These retrograde fluids may also have triggered new zircon growth, or the partial resorption of narrow zircon rims as suggested by the embayed rim morphologies. Unfortunately, the very narrow and delicate nature of these overgrowths makes isotopic analysis virtually impossible with current techniques. It may be significant that these overgrowths have only been recognized in BSE images of thin sections. Such narrow and discontinuous overgrowths are unlikely to survive sample crushing and mineral separation techniques.

Zone V and higher grades

A distinct change in zircon morphology is evident in Zone V samples (gf-99-98, gf-99-128), where zircons appear as euhedral grains, showing well-defined and undamaged crystal faces and in some cases pointed terminations (Fig. 7). This is similar to the observations of Williams (2001) from the Cooma Complex of SE Australia, where new growth of zircon at migmatite grade occurs preferentially as pyramidal overgrowths on pre-existing grains, and of Rubatto *et al*. (2001), who found new zircon growth restricted to the partial-melting zone in the Reynolds Range of central Australia. There is no evidence in Zone V of the narrow irregular rims seen from inner Zone I to Zone III. It is not clear whether this is due to progressive increase in zircon precipitation resulting in complete overgrowth of cores, or to dissolution of the narrow low-grade zircon rims, followed by reprecipitation of zircon as grain terminations at migmatite grade.

U–Pb isotopic analyses of migmatite zircons

Six fractions of zircon from two migmatite-grade samples were analysed for U–Pb isotopic composition (Fig. 8). Five of the six fractions come from sample gf-99-128, collected from a metasedimentary screen included within granite of the Ballachulish Igneous Complex on the eastern side of the igneous complex (Fig. 1). Zircons were separated from three lithological components from this sample: (1) coherent pelitic rock fragments; (2) ductile K-feldspar-rich layers interpreted as local partial melt segregations; (3) granodiorite injected from the surrounding

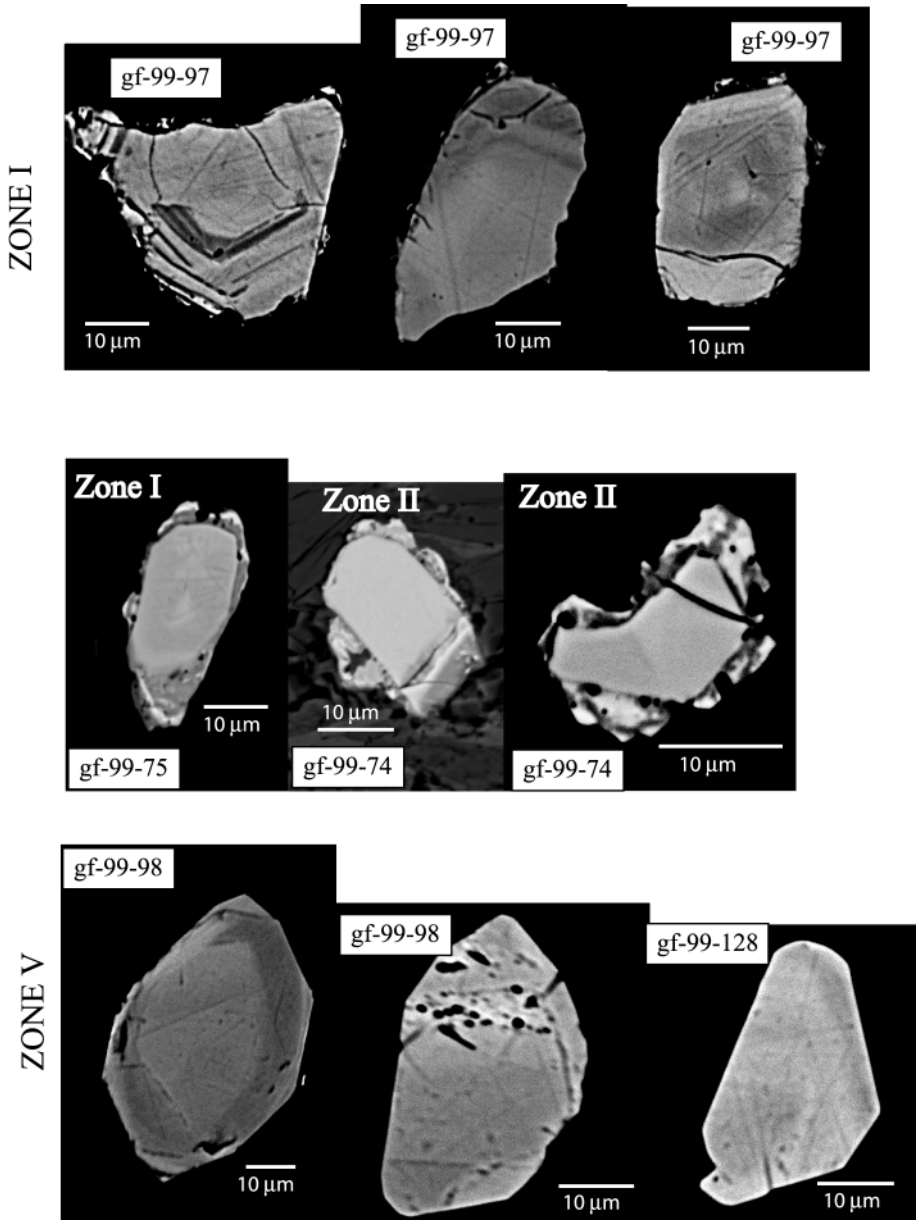

Fig. 7. BSE images of zircons in thin section in metapelitic rocks from the Ballachulish thermal aureole. All samples come from the SW part of the aureole, where host rocks are schists of the Creran succession, Argyll Group. The material forming discontinuous, embayed rims on zircons in Zones I and II is also zircon.

igneous complex. The sixth fraction comes from sample 92-B-43B, from the SW part of the thermal aureole in the upper part of Zone V. This sample contains garnet, making it one of the highest-grade samples collected within the aureole, probably having reached >750 °C.

All six zircon fractions from the migmatites show isotopic evidence of extensive zircon inheritance. All analyses are more than 10% discordant, and all are hundreds of millions of years older than the age of the Ballachulish Igneous Complex. These six analyses do not define a single mixing line, but suggest the presence of inherited zircon components with a variety of ages. Given the lack of well-defined mixing lines, and the possibility of multistage Pb loss as well as new zircon growth in association with Ballachulish contact metamorphism, it is not possible to place firm constraints on the age of inherited (presumably detrital) zircons based on these analyses. However, the inherited components appear to be at least Grenvillian in age, and mixing lines to *c*. 427 Ma extrapolate back to as old as *c*. 1400 Ma. It is noteworthy that there is no evidence in these analyses, nor from the inherited components in the Ballachulish Granite or Glencoe rhyolite, for any Knoydartian (800–870 Ma) zircon component, as proposed by Prave (1999) as a source for Dalradian metasediments, although many more analyses are needed to thoroughly test this idea.

In summary, zircon in the Ballachulish aureole is dominated by inherited, detrital grains, with volumetrically minor new growth occurring at migmatite grade, similar to observations from other progressive low-pressure metapelitic sequences (Rubatto *et al*. 2001; Williams 2001). We also observe very fine rims of apparent new zircon of enigmatic origin at lower grade in the aureole.

Monazite in the Ballachulish aureole

Zone I

Monazite was observed in samples from Zone I in the aureole, outside of the first development of cordierite (Zone II). In the

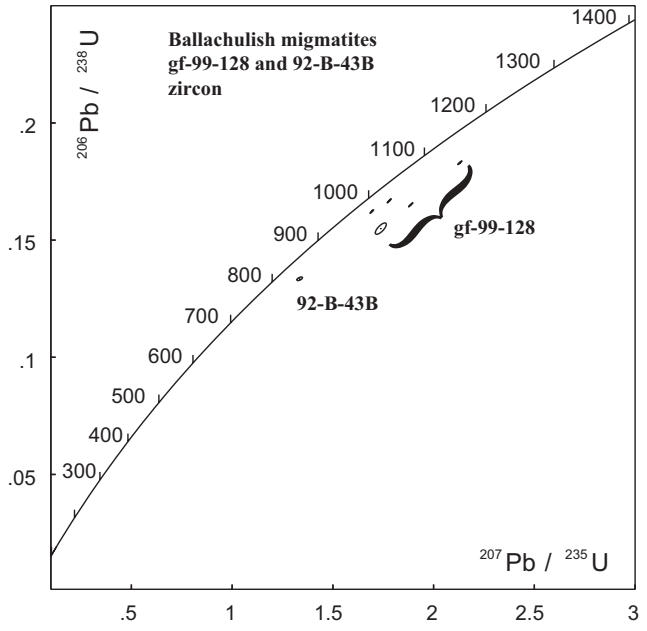

Fig. 8. U–Pb concordia diagram showing zircon analyses from migmatite samples gf-99-128 and 92-B-43B.

outer part of Zone I (sample gf-99-97), monazite occurs as ragged, anhedral grains, with deep embayments (Fig. 9a-c). These grains are up to a few tens of microns long, and tend to occur in groups. Monazite is also found partly enveloping cores of apatite (Fig. 9d). At slightly higher grade, in the inner part of Zone I, some of the monazite is similar to that seen at lower grade (Fig. 9h) but it is proportionately less abundant. Monazite also occurs as very fine wisps along mica cleavages (Fig. 9g) and as elongate, anhedral grains aligned with the mica foliation (Fig. 9e). One example was found of monazite intimately intergrown with a larger host grain of iron oxide (Fig. 9f).

Zone III and higher grades

A marked change in monazite morphology is observed between samples in Zone I and those in Zone III and upgrade. This change occurs in the temperature interval 560–600 °C, and coincides with the onset of dehydration reactions involving chlorite and muscovite breakdown. Within Zones III–V, monazite occurs in greater abundance than in Zone I, but rather than occurring as distinct grains, it occurs as clusters of tiny (typically 4–6 μm) ovoid blebs (Fig. 9j–o). The lowest-grade sample in which these monazite clusters has been found is gf-99-77, from Zone III in the aureole. They are particularly abundant in Zones IV and V. These monazite clusters have the appearance of pseudomorphs after some tabular precursor, although no remnants have been found of a likely pre-existing pseudomorphed phase (e.g. allanite, apatite) associated with these clusters. Monazite clusters occur in a variety of host minerals, including cordierite, quartz, biotite and andalusite.

Further upgrade, within the migmatitic portion of Zone V, monazite occurs as elongate trails of ovoid blebs (Fig. 9p–r). We interpret these to be of similar origin to the monazite clusters described above, but to have been disrupted and smeared out during minor ductile deformation of the melt-bearing migmatites.

Discussion of monazite textures

The very fine grain size of monazite throughout the aureole has foiled attempts to separate monazite from these rocks for isotopic analysis, and thus the discussion below is limited to interpretations of textures seen in thin section. In none of the rocks through the metamorphic sequence is monazite completely absent. This contrasts with the common view of a monazite stability 'gap' between lower greenschist and mid-amphibolite facies (Overstreet 1967).

The simplest explanation for the origin of most of the monazite seen in outer Zone I is that it is detrital, although without age information we cannot be certain. The deeply embayed morphology of most grains in Zone I is suggestive of partial resorption of pre-existing (detrital) grains, although this morphology is also reminiscent of those illustrated by Rasmussen *et al*. (2001), which they interpreted to record low-grade (prehnite–pumpellyite facies) metamorphism. The apparent decrease in monazite abundance from the outer to the inner parts of Zone I is consistent with monazite being mineralogically unstable at P–T conditions below *c*. 550 °C and 3 kbar during contact metamorphism. The fine wisps of monazite seen along mica cleavage in the upper part of Zone I (Fig. 9g) may be indicative of monazite dissolution and transport.

Lower amphibolite-grade regional metamorphism predating intrusion of the Ballachulish Igneous Complex may have resulted in some monazite growth. This may be the origin of textures such as shown in Figure 9d, where monazite partially surrounds an apatite core. The tiny grains of monazite included within iron oxide seen in sample gf-99-75 (Fig. 9f) suggest another possible origin for some monazite. Rubatto *et al*. (2001) also identified very small monazite grains in the core of Fe–Ti oxide aggregates in greenschist-facies samples from the Reynolds Range, central Australia.

The most distinct feature of monazite in the Ballachulish aureole is the morphological and textural difference between monazites in Zone I and those in Zones III, IV and V. Whereas in Zone I monazite exhibits a variety of morphologies and mineral associations, in Zones III, IV and V monazite occurs exclusively as clusters or trails of tiny, ovoid blebs. This distinct grade-related change occurs in an interval marked first by a decrease in chlorite and increase in cordierite abundance (Zones II and III) and then the incoming of K-feldspar (Zone IV). The temperature interval for these changes is *c*. 560 to 600 °C. Similar monazite textures are seen in the Ballachulish Slate in samples from Zones III, IV and V, which, despite a slightly different reaction history as a result of bulk compositional effects (see Pattison & Harte 1997 for summary), have experienced chlorite breakdown and cordierite growth in Zones II and III.

The textural change with metamorphic grade could result from either recrystallization of pre-existing monazite, or entirely new growth. However, the increased abundance of monazite in Zones III, IV and V relative to Zone I and its occurrence in clusters rather than as embayed grains are suggestive of new growth. In either case, the expectation would be that monazites from Zones III, IV and V would record the age of contact metamorphism, although we have not been able to test this given the very small grain size of individual monazite blebs.

Comparison with other settings

The apparent critical temperature between 560 to 600 °C for monazite growth at Ballachulish is broadly consistent with several previous studies of monazite in prograde metamorphic

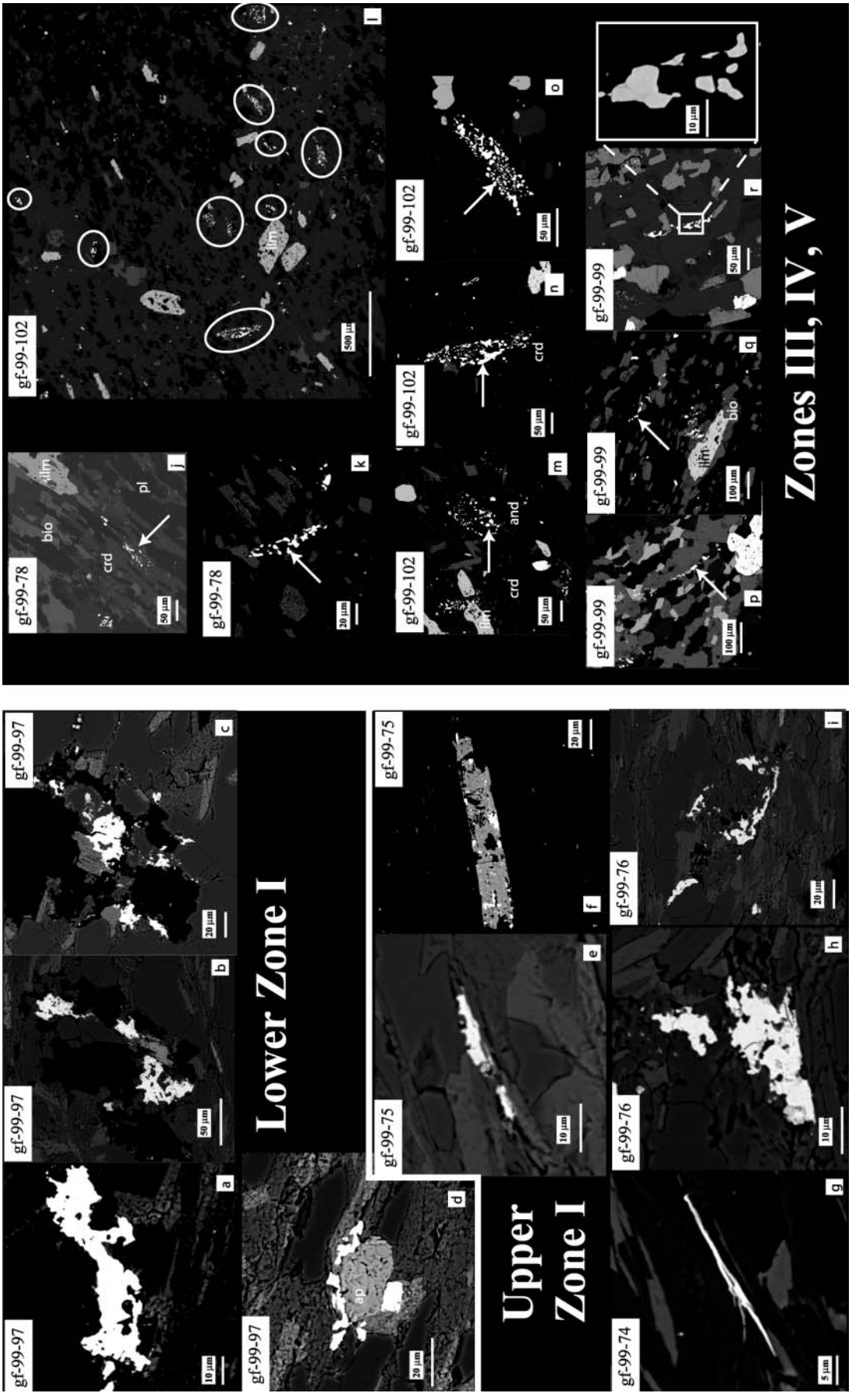

Fig. 9. BSE images of monazites in thin section in metapelitic rocks from the Ballachulish thermal aureole. All samples are from the SW part of the aureole as shown in Figure 6. Images are presented in order of increasing metamorphic grade through the aureole. Lower Zone I: (**a**)–(**c**) relatively large, deeply embayed monazite; (**d**) monazite surrounding apatite. Upper Zone I: (**e**) elongate, anhedral monazite aligned with mica foliation; (**f**) monazite inclusions in iron oxide; (**g**) very fine, wispy monazite found within mica cleavage; (**h**), (**i**) deeply embayed, anhedral monazite. Zones III, IV and V: (**j**)–(**o**) examples of tiny, ovoid monazites occurring in clusters suggestive of a larger, pre-existing grain. Circles in (**l**) highlight clusters of monazite. (**p**)–(**r**) monazite trails in migmatite interpreted as mildly deformed equivalents of the monazite clusters seen at slightly lower grade. and, andalusite; ap, apatite; bio, biotite; crd, cordierite; ilm, ilmenite; pl, plagioclase. Arrows point to monazite clusters and trails.

sequences. Rubatto *et al*. (2001) reported the first appearance of monazite of demonstrably metamorphic origin at temperatures between 500 and 600 °C, at *c*. 5 kbar, although specific isograd reactions were not discussed. Williams (2001) found metamorphic monazite at the K-feldspar-in isograd (*c*. 600 °C, *c*. 4 kbar). Wing *et al*. (2003) reported an allanite to monazite isograd coinciding with the aluminosilicate-in isograd from both Buchan- and Barrovian-style terranes and a contact aureole from northern New England, USA. Those workers presented monazite textures similar to those seen in the Ballachulish aureole, with irregular embayed grains at chlorite grade, giving way to clusters of small ovoid grains at grades above the andalusite or kyanite isograd. In contrast to our observations at Ballachulish, Wing *et al*. (2003) also found a distinct zone of euhedral allanite between the biotite and aluminosilicate-in isograds and they proposed a prograde reaction sequence in which detrital monazite is consumed to form allanite, which in turn reacts at higher metamorphic grade to form clusters of metamorphic monazite.

Kingsbury *et al*. (1993) also reported textures very similar to those in the high-grade parts of the Ballachulish aureole, in which monazite occurs as 'trains' roughly parallel to the foliation. Kingsbury *et al*. (1993) reported metamorphic monazite to first appear in staurolite–garnet-bearing rocks at temperatures of 550 ± 50 °C. At lower grade (*c*. 400–540 °C), Kingsbury *et al*. (1993) found a texture remarkably similar to the monazite clusters seen in Zone IV at Ballachulish (compare Fig. 9l with Kingsbury *et al*. 1993, fig. 4). However, Kingsbury *et al*. (1993) reported this texture to be formed by a Ce-poor phosphate that they interpreted to have replaced allanite and to be a precursor to metamorphic monazite. At Ballachulish we see no evidence for a Ce-poor phosphate. All the grains in Figure 9 have typical monazite compositions with Ce_2O_3 contents ranging between 26 and 30%.

Wing *et al*. (2003) documented a distinct zone of euhedral allanite between the biotite and aluminosilicate isograds and proposed a prograde reaction sequence in which detrital monazite is consumed at the biotite isograd to form allanite, which in turn reacts at the aluminosilicate isograd to form clusters of metamorphic monazite. The suggestion of allanite as a monazite precursor has also been made by Overstreet (1967) and Smith & Barreiro (1990). Finger *et al*. (1998) reported the reverse relationship, in which igneous monazite reacted to form secondary apatite, allanite and epidote at amphibolite-facies conditions. No allanite has been found in the Ballachulish aureole. The allanite zone of Wing *et al*. (2003) would correspond to Zones II and III at Ballachulish (i.e. between the biotite and andalusite isograds), although we find apparent metamorphic monazite below the andalusite isograd in sample gf-99-77. Wing *et al*. (2003) suggested that cordierite or staurolite could play the same role as andalusite or kyanite in a monazite-producing reaction. This may explain the presence of monazite at Ballachulish in cordierite-bearing rocks of Zone III. If this is the case, allanite may be restricted to a very narrow region corresponding to Zone II in the aureole. Alternatively, Spear & Pyle (2002) and Wing *et al*. (2003) have shown that bulk-rock Ca and Al content is important in determining the stability of allanite v. monazite in pelitic rocks. Some combination of these factors might explain why we have not observed allanite at Ballachulish, and why monazite appears to have grown below the aluminosilicate isograd.

In summary, monazite in the Ballachulish aureole shows a distinct change in morphology and increase in abundance across the cordierite zone, suggestive of new metamorphic monazite growth at temperatures between *c*. 560 and 600 °C. The textures suspected of representing new monazite growth have not been dated because of the small grain size, and without this critical test our textural interpretations remain subject to uncertainty. However, several other studies of prograde pelitic metamorphic sequences present broadly similar observations, with metamorphic monazite forming at, or close to, the aluminosilicate (andalusite or kyanite) isograd. Monazite therefore appears to be more sensitive to metamorphism than zircon, which typically does not grow below migmatite grade in pelitic rocks. Consequently, we suggest that monazite is a better target than zircon for U–Pb geochronology of metamorphism in upper amphibolite-facies rocks that have not experienced partial melting.

This work was supported by NSERC grants to D.R.M.P. (0037233) and L.M.H. (170087), and a Killam post-doctoral research award from the University of Calgary (to G.L.F.). A. Bergren, K. Toope, L. Rayner and S. Hagen assisted with various aspects of mineral separation, chemistry and mass spectrometry at the University of Alberta. L. Shi assisted with BSE imaging and electron probe analyses. We thank F. Spear and B. Harte for constructive reviews, and M. Whitehouse for helpful editorial handling.

References

Bailey, E.B. & Maufe, H.B. 1960. *The geology of Ben Nevis and Glencoe and the Surrounding Country: Explanation of Sheet 53, 2nd*. Memoirs of the Geological Society of Scotland, HMSO, Edinburgh.

Brown, P.E., Miller, J.A. & Grasty, R.L. 1968. Isotopic ages of late-Caledonian granitic intrusions in the British Isles. *Proceedings of the Yorkshire Geological Society*, **36**, 251–276.

Buntebarth, G. 1991. Thermal models of cooling. *In:* Voll, G., Topel, J., Pattison, D.R.M. & Seifert, F. (eds) *Equilibrium and Kinetics in Contact Metamorphism: The Ballachulish Igneous Complex and its Aureole*. Springer, Berlin, 181–210.

Cherniak, D.J., Watson, E.B., Harrison, T.M. & Grove, M. 2000. Pb diffusion in monazite: a progress report on a combined RBS/SIMS study. *EOS Transactions, American Geophysical Union*, **41**, S25.

Clayburn, J.A.P., Harmon, R.S., Pankhurst, R.J. & Brown, J.F. 1983. Sr, O and Pb isotope evidence for the origin and evolution of the Etive Igneous Complex, Scotland. *Nature*, **303**, 492–497.

Clough, C.T.H., Maufe, H.B. & Bailey, E.B. 1909. The cauldron subsidence of Glencoe and associated igneous phenomena. *Quarterly Journal of the Geological Society of London*, **65**, 611–678.

Degeling, H., Eggins, S. & Ellis, D.H. 2001. Zr budgets for metamorphic reactions, and the formation of zircon from garnet breakdown. *Mineralogical Magazine*, **65**(6), 749–758.

Dempster, T.J. 1985. Uplift patterns and orogenic evolution in the Scottish Dalradian. *Journal of the Geological Society, London*, **142**, 111–128.

Droop, G.T.R. & Treloar, P.J. 1981. Pressure of metamorphism in the thermal aureole of the Etive Granite Complex. *Scottish Journal of Geology*, **17**, 85–102.

Ferry, J.M. 1996a. Three novel isograds in metamorphosed siliceous dolomites from the Ballachulish aureole, Scotland. *American Mineralogist*, **81**, 485–494.

Ferry, J.M. 1996b. Prograde and retrograde fluid flow during contact metamorphism of siliceous carbonates from the Ballachulish aureole, Scotland. *Contributions to Mineralogy and Petrology*, **124**, 235–254.

Finger, F., Broska, I., Roberts, M. & Schermaier, A. 1998. Replacement of primary monazite by apatite–allanite–epidote coronas in an amphibolite-facies granite gneiss from the Eastern Alps. *American Mineralogist*, **83**(3-4), 248–258.

Fraser, G., Ellis, D. & Eggins, S. 1997. Zirconium abundance in granulite-facies minerals, with implications for zircon geochronology in high-grade rocks. *Geology*, **25**, 607–610.

Harte, B., Pattison, D.R.M. & Linklater, C.M. 1991. Field relations and petrography of partially melted pelitic and semi-pelitic rocks. *In:* Voll, G., Topel, J., Pattison, D.R.M. & Seifert, F. (eds) *Equilibrium and Kinetics in Contact Metamorphism: the Ballachulish Igneous Complex and its Aureole*. Springer, Berlin, 181–210.

Haslam, H.W. & Kimbell, G.S. 1981. *Disseminated Copper–Molybdenum Mineralisation near Ballachulish, Highland Region*. Reconnaissance Programme Report, Institute of Geological Sciences, London, **43**.

Heaman, L.M. & LeCheminant, A.N. 1993. Paragenesis and U–Pb systematics of baddeleyite (ZrO_2). *Chemical Geology*, **110**, 95–126.

HEAMAN, L.M. & TARNEY, J. 1989. U–Pb baddeleyite ages for the Scourie dyke swarm, Scotland; evidence for two distinct intrusion events. *Nature*, **340**(6236), 705–708.

HEAMAN, L.M., ERDMER, P. & OWEN, J.V. 2002. U–Pb geochronologic constraints on the crustal evolution of the Long Range Inlier, Newfoundland. *Canadian Journal of Earth Sciences*, **39**, 845–865.

HOERNES, S., MACLEOD-KINSELL, S., HARMON, R.S., PATTISON, D.R.M. & STRONG, D.F. 1991. Stable isotope geochemistry on the intrusive complex and its metamorphic aureole. *In:* VOLL, G., TOPEL, J., PATTISON, D.R.M. & SEIFERT, F. (eds) *Equilibrium and Kinetics in Contact Metamorphism: the Ballachulish Igneous Complex and its Aureole*. Springer, Berlin, 351–375.

JACQUES, J.M. & REAVY, R.J. 1994. Caledonian plutonism and major lineaments in the SW Scottish Highlands. *Journal of the Geological Society, London*, **151**, 955–969.

KATO, A. & MATSUBARA, S. 1991. Geikielite, baddeleyite and zirconolite in dolomitic marble from the Neichi mine, Miyoko City, Iwate Prefecture, Japan. *Bulletin of the National Science Museum, Tokyo, Series C*, **17**, 11–20.

KINGSBURY, J.A., MILLER, C.F., WOODEN, J.L. & HARRISON, T.M. 1993. Monazite paragenesis and U–Pb systematics in rocks of the eastern Mojave Desert, California, U.S.A.: implications for thermochronometry. *Chemical Geology*, **110**, 147–167.

LECHEMINANT, A.N. & HEAMAN, L.M. 1989. Mackenzie igneous events, Canada: middle Proterozoic hotspot magmatism associated with ocean opening. *Earth and Planetary Science Letters*, **96**(1-2), 38–48.

MILLER, J.A. & BROWN, P.E. 1965. Potassium–argon age studies in Scotland. *Geological Magazine*, **102**, 106–134.

MOORE, I. & KOKELAAR, P. 1998. Tectonically controlled piecemeal caldera collapse: a case study of Glencoe volcano, Scotland. *Geological Society of America Bulletin*, **110**(11), 1448–1466.

OVERSTREET, W.C. 1967. *The Geologic Occurrence of Monazite*. US Geological Survey, Professional Paper, **530**.

PATTISON, D.R.M. 1989. *P–T* conditions and the influence of graphite on pelitic phase relations in the Ballachulish aureole, Scotland. *Journal of Petrology*, **30**, 1219–1244.

PATTISON, D.R.M. 1992. Stability of andalusite and sillimanite and the Al_2SiO_5 triple point: constraints from the Ballachulish aureole, Scotland. *Journal of Geology*, **100**, 423–446.

PATTISON, D.R.M. & HARTE, B. 1988. Evolution of structurally contrasting anatectic migmatites in the 3 kbar Ballachulish aureole, Scotland. *Journal of Metamorphic Geology*, **6**, 475–494.

PATTISON, D.R.M. & HARTE, B. 1991. Petrography and mineral chemistry of pelites. *In:* VOLL, G., TOPEL, J., PATTISON, D.R.M. & SEIFERT, F. (eds) *Equilibrium and Kinetics in Contact Metamorphism: the Ballachulish Igneous Complex and its Aureole*. Springer, Berlin, 135–180.

PATTISON, D.R.M. & HARTE, B. 1997. The geology and evolution of the Ballachulish Igneous Complex and Aureole. *Scottish Journal of Geology*, **33**, 1–29.

PATTISON, D.R.M. & HARTE, B. 2001. *The Ballachulish Igneous Complex and Aureole: a Field Guide*. Edinburgh Geological Society, Edinburgh.

PATTISON, D.R.M. & VOLL, G. 1991. Regional geology of the Ballachulish area. *In:* VOLL, G., TOPEL, J., PATTISON, D.R.M. & SEIFERT, F. (eds) *Equilibrium and Kinetics in Contact Metamorphism: the Ballachulish Igneous Complex and its Aureole*. Springer, Berlin, 19–38.

PRAVE, A.R. 1999. The Neoproterozoic Dalradian Supergroup of Scotland: an alternative hypothesis. *Geological Magazine*, **136**, 609–617.

PURTSCHELLER, F. & TESSADRI, R. 1985. Zirconolite and baddeleyite from metacarbonates of the Otzal–Stubai complex (northern Tyrol, Austria). *Mineralogical Magazine*, **49**, 523–529.

PYLE, J.M. & SPEAR, F.S. 1999. Yttrium zoning in garnet: coupling of major and accessory phases during metamorphic reactions. *Geological Materials Research*, **1**(6), 1–49.

RASMUSSEN, B., FLETCHER, I.R. & MCNAUGHTON, N.J. 2001. Dating low-grade metamorphic events by SHRIMP U–Pb analysis of monazite in shales. *Geology*, **29**(10), 963–966.

ROGERS, G. & DUNNING, G.R. 1991. Geochronology of appinitic and related granitic magmatism in the W Highlands of Scotland: constraints on the timing of transcurrent fault movement. *Journal of the Geological Society, London*, **148**, 17–27.

RUBATTO, D., WILLIAMS, I.S. & BUICK, I.S. 2001. Zircon and monazite response to prograde metamorphism in the Reynolds Range, central Australia. *Contributions to Mineralogy and Petrology*, **140**, 458–468.

SMITH, H.A. & BARREIRO, B. 1990. Monazite U–Pb dating of staurolite grade metamorphism in pelitic schists. *Contributions to Mineralogy and Petrology*, **105**, 602–615.

SMITH, H.A. & GILETTI, B.J. 1997. Lead diffusion in monazite. *Geochimica et Cosmochimica Acta*, **61**, 1047–1055.

SPEAR, F.S. & PYLE, J.M. 2002. Apatite, monazite and xenotime in metamorphic rocks. *In:* KOHN, M.J., RAKOVAN, J. & HUGHES, J.M. (eds) *Phosphates: Geochemical, Geobiological, and Materials Importance*. Mineralogical Society of America, Reviews in Mineralogy and Geochemistry, **48**, 293–335.

STEPHENSON, D. & GOULD, D. 1995. *British Regional Geology: the Grampian Highlands*, *4th*. HMSO, London.

STEWART, M., STRACHAN, R.A. & HOLDSWORTH, R.E. 1999. Structure and early kinematic history of the Great Glen Fault Zone, Scotland. *Tectonics*, **18**, 326–342.

STEWART, M., STRACHAN, R.A., MARTIN, M.W. & HOLDSWORTH, R.E. 2001. Constraints on early sinistral displacements along the Great Glen Fault Zone, Scotland: structural setting, U–Pb geochronology and emplacement of the syn-tectonic Clunes tonalite. *Journal of the Geological Society, London*, **158**, 821–830.

TAUBENECK, W. 1967. Notes on the Glencoe cauldron subsidence, Argyllshire, Scotland. *Geological Society of America Bulletin*, **78**, 1295–1316.

THIRLWALL, M.F. 1988. Geochronology of Late Caledonian magmatism in northern Britain. *Journal of the Geological Society, London*, **145**, 951–967.

TROLL, G. & WEISS, S. 1991. Structure, petrography and emplacement of plutonic rocks. *In:* VOLL, G., TOPEL, J., PATTISON, D.R.M. & SEIFERT, F. (eds) *Equilibrium and Kinetics in Contact Metamorphism: the Ballachulish Igneous Complex and its Aureole*. Springer, Berlin, 39–66.

VOLL, G., TOPEL, J., PATTISON, D.R.M. & SEIFERT, F. (EDS) 1991. *Equilibrium and Kinetics in Contact Metamorphism: The Ballachulish Igneous Complex and its Aureole*. Springer, Berlin.

WEISS, S. 1986. *Petrogenese des Intrusivkomplexes von Ballachulish, Westschottland: Kristallisationsverlauf in einen zonierten Kaledonischen Pluton*. PhD thesis, Ludwig-Maximilians-Universität, Munich.

WEISS, S. & TROLL, G. 1989. The Ballachulish Igneous Complex, Scotland: petrography, mineral chemistry and order of crystallization in the monzodiorite–quartz diorite suite and in the granite. *Journal of Petrology*, **30**, 1069–1116.

WILLIAMS, I.S. 2001. Response of detrital zircon and monazite, and their U–Pb isotopic systems, to regional metamorphism and host-rock partial melting, Cooma Complex, southeastern Australia. *Australian Journal of Earth Sciences*, **48**, 557–580.

WING, B.A., FERRY, J.M. & HARRISON, T.M. 2003. Prograde destruction and formation of monazite and allanite during contact and regional metamorphism of pelites: petrology and geochronology. *Contributions to Mineralogy and Petrology*, **145**, 228–250.

WINGATE, M.T.D., CAMPBELL, I.H. & HARRIS, L.B. 2000. SHRIMP baddeleyite age for the Fraser dyke swarm, Southeast Yilgarn Craton, Western Australia. *Australian Journal of Earth Sciences*, **47**(2), 309–313.

Received 3 February 2003; revised typescript accepted 3 September 2003.
Scientific editing by Martin Whitehouse